

**STYLIZED BENCHMARK DESCRIPTION AND REFERENCE  
SOLUTIONS FOR THE PIN-FUELED SMALL MODULAR  
ADVANCED HIGH TEMPERATURE REACTOR**

A Thesis  
Presented to  
The Academic Faculty

by

Kristina Elisabeth Reed

In Partial Fulfillment  
of the Requirements for the Degree  
Master of Science in Nuclear Engineering in the  
George W. Woodruff School of Mechanical Engineering

Georgia Institute of Technology  
May 2021

**COPYRIGHT © 2021 BY KRISTINA ELISABETH REED**

**STYLIZED BENCHMARK DESCRIPTION AND REFERENCE  
SOLUTIONS FOR THE PIN-FUELED SMALL MODULAR  
ADVANCED HIGH TEMPERATURE REACTOR**

Approved by:

Dr. Farzad Rahnema, Advisor  
George W. Woodruff School  
*Georgia Institute of Technology*

Dr. Dan Ilas  
Consultant

Dr. Dingkang Zhang  
George W. Woodruff School  
*Georgia Institute of Technology*

Dr. Bojan Petrovic  
George W. Woodruff School  
*Georgia Institute of Technology*

Date Approved: November 23<sup>rd</sup>, 2020

## **ACKNOWLEDGEMENTS**

I would like to thank Dr. Farzad Rahnema, Dr. Dinkang Zhang, and Dr. Dan Ilas for their guidance on this work as well as Dr. Bojan Petrovic for serving on my committee. The feedback and advice I received from them were valuable for both the thoroughness of this work and my own development as a graduate researcher. Additionally, I would like to thank the DOE Office of Nuclear Energy's Nuclear Energy University Program for funding my research under the United States Department of Energy Integrated University Program Graduate Fellowship.

# TABLE OF CONTENTS

<b>ACKNOWLEDGEMENTS</b>	<b>iii</b>
<b>LIST OF TABLES</b>	<b>v</b>
<b>LIST OF FIGURES</b>	<b>vi</b>
<b>LIST OF SYMBOLS AND ABBREVIATIONS</b>	<b>vii</b>
<b>SUMMARY</b>	<b>viii</b>
<b>CHAPTER 1. Introduction</b>	<b>1</b>
<b>CHAPTER 2. Summary of ORNL Preconceptual Design Specifications</b>	<b>3</b>
2.1 Radial Layout	3
2.2 Axial Layout	4
2.3 Assembly Specifications	5
2.4 Fuel Composition	6
<b>CHAPTER 3. Stylized Benchmark Specifications</b>	<b>8</b>
3.1 Coolant Channel Modifications	8
3.2 Burnable Poison Content	9
3.3 Control Rods	11
3.3.1 Control Rod Placement A	12
3.3.2 Control Rod Placement B	13
3.3.3 Control Rod Placement C	14
3.4 TRISO Fuel	15
3.5 Stylized Core Specifications	17
3.5.1 Stylized Radial Layout	17
3.5.2 Stylized Axial Layout	18
3.5.3 Geometric and Material Specifications	19
<b>CHAPTER 4. Benchmark Results</b>	<b>22</b>
4.1 Results Summary	22
4.2 Radial Fission Density Distribution Results	25
4.3 Axial Fission Density Distribution Results	31
4.4 Assembly-Averaged 11-Division Relative Fission Density Results	33
<b>CHAPTER 5. Future Work</b>	<b>43</b>
<b>APPENDIX A. SUMMARY OF ATTACHED FILES</b>	<b>44</b>
A.1 Input Files	44
A.2 Data Files	45
<b>REFERENCES</b>	<b>47</b>

## LIST OF TABLES

Table I. Geometric Specifications.....	20
Table II. Material Specifications.....	21
Table III. Comparison of Stylized Benchmark Criticality Results .....	24
Table IV. 1/11 <sup>th</sup> Assembly-Avg. Relative Fission Densities - Uncontrolled Core A.....	35
Table V. 1/11 <sup>th</sup> Assembly-Avg. Relative Fission Densities - Controlled Core – A .....	36
Table VI. 1/11 <sup>th</sup> Assembly-Avg. Relative Fission Densities - Near-Critical Core – A ....	37
Table VII. 1/11 <sup>th</sup> Assembly-Avg. Relative Fission Densities - Uncontrolled Core – B...	38
Table VIII. 1/11 <sup>th</sup> Assembly-Avg. Relative Fission Densities - Controlled Core – B .....	39
Table IX. 1/11 <sup>th</sup> Assembly-Avg. Relative Fission Densities - Near-Critical Core – B ....	40
Table X. 1/11 <sup>th</sup> Assembly-Avg. Relative Fission Densities - Uncontrolled Core – C .....	41
Table XI. 1/11 <sup>th</sup> Assembly-Avg. Relative Fission Densities - Controlled Core – C .....	42
Table XII. Input File Summary.....	44
Table XIII. Data File Summary .....	45

## LIST OF FIGURES

Figure 1. Original SmAHTR Core Cross Section <sup>1</sup> .....	4
Figure 2. SmAHTR Axial Schematic from ORNL Report <sup>1</sup> .....	5
Figure 3. SmAHTR Cylindrical Fuel Pin Assembly .....	6
Figure 4. Original Assembly (Left) and Modified Assembly (Right) .....	9
Figure 5. Stylized Assembly Before (Left) and After Addition of Burnable Poison Rods (Right) .....	10
Figure 6. Control Rod Placement A.....	13
Figure 7. Control Rod Placement B .....	14
Figure 8. Control Rod Placement C .....	15
Figure 9. TRISO Composition.....	15
Figure 10. Stylized SmAHTR Core Cross Section for Control Rod Placement A.....	18
Figure 11. Control Rod Pattern for Near-Critical Core – Control Rod Option A .....	23
Figure 12. Control Rod Pattern for Near-Critical Core – Control Rod Option B.....	23
Figure 13. Assembly Pin Indices .....	25
Figure 14. Radial Fission Density Distribution for Controlled (Left) and Uncontrolled (Right) Assembly A .....	26
Figure 15. Radial Fission Density Distribution for Controlled (Left) and Uncontrolled (Right) Assembly B .....	27
Figure 16. Radial Fission Density Distribution for Controlled (Left) and Uncontrolled (Right) Assembly C .....	27
Figure 17. Radial Fission Density Distribution for Controlled (Left) and Uncontrolled (Right) Core A .....	29
Figure 18. Radial Fission Density Distribution for Controlled (Left) and Uncontrolled (Right) Core B.....	29
Figure 19. Radial Fission Density Distribution for Controlled (Left) and Uncontrolled (Right) Core C.....	30
Figure 20. Radial Fission Density Distribution for Near-Critical Core A (Left) and Near-Critical Core B (Right).....	30
Figure 21. Axial Fission Density Distribution for Core A.....	32
Figure 22. Axial Fission Density Distribution for Core B.....	32
Figure 23. Axial Fission Density Distribution for Core C.....	33
Figure 24. Stylized Core Cross Section with Assembly Indices .....	34

## LIST OF SYMBOLS AND ABBREVIATIONS

2-D	Two-Dimensional
3-D	Three-Dimensional
AGR	Advance Gas Reactor
AHTR	Advanced High Temperature Reactor
BP	Burnable Poison
DRACS	Direct Reactor Auxiliary Cooling System
FHR	Fluoride-Salt-Cooled High-Temperature Reactor
FLiBe	<sup>7</sup> Li-Enriched salt coolant in 2:1 <sup>7</sup> LiF to BeF <sub>2</sub> ratio
HTTR	High Temperature Test Reactor
$k_{\text{eff}}$	k-effective: eigenvalue for reactor criticality incorporating leakage
LEU	Low-Enriched Uranium
MCNP	Monte Carlo N-Particle Transport Code
ORNL	Oak Ridge National Laboratory
pcm	Per cent mille – One thousandth of a percent (relative uncertainty * 10 <sup>5</sup> )
PHX	Primary Heat Exchanger
PyC	Pyrolytic Carbon
SmAHTR	Small modular Advanced High-Temperature Reactor
SMR	Small Modular Reactor
TRISO	Tri-Structural Isotropic Fuel
UCO	Uranium Oxycarbide
VHTR	Very High Temperature Reactor
VPF	Volumetric Packing Fraction

## SUMMARY

This thesis provides detailed, stylized neutronic steady-state benchmark problems and solutions based on the Oak Ridge National Laboratory (ORNL) preconceptual design of a fluoride-salt-cooled Small modular Advanced High Temperature Reactor (SmAHTR).<sup>1</sup> The SmAHTR preconceptual design details a small scale, transportable reactor of 19 prismatic assemblies which utilize tri-isotropic (TRISO) particles of Uranium Oxide (UCO) in pin-type graphite compacts for fuel. This set of stylized benchmark problems addresses several outstanding design gaps while preserving the desired reactor characteristics (high heterogeneity, small-scale, thermal hydraulic performance) of the preconceptual design.

First in this thesis, the cylindrical pin-type-fueled preconceptual SmAHTR design is detailed below as it is originally specified in the ORNL report.<sup>1</sup> Then, the necessary modifications are made to address the outstanding design gaps of the preconceptual design. The gaps addressed in this paper include the modification of the coolant channel to reduce bypass flow, the addition of burnable poison (BP) to extend cycle length and achieve a realistic power distribution, and the inclusion of control rods to maintain criticality or shutdown the reactor. Each of these modifications to address gaps in the preconceptual design are thoroughly detailed, and three options are presented for the addition of control rods. Each of the three control rod placement options are detailed with exact geometric and material specifications, and they are presented in uncontrolled (control rods fully withdrawn) and controlled (control rods fully inserted) configurations for both the full core and single assembly cases. A section is devoted to the fuel composition since the exact

composition is not explicitly specified in the preconceptual report, and details and considerations for the TRISO packing structure are discussed. The geometric specifications for the stylized benchmark problems are then presented with any assumptions made axially or radially, and three-dimensional (3-D) single assembly and full core variants are fully detailed. All material specifications including temperature, density, atomic composition, and data library are provided for the stylized benchmark set. These stylized descriptions include all specifications necessary for creating neutronic benchmark problems based on the preconceptual design, and continuous energy Monte Carlo code MCNP5<sup>2</sup> reference solutions for the eigenvalues ( $k_{\text{eff}}$ ), radial fission density distributions, axial fission density distributions, and assembly-averaged fission densities in each axial division of the core are provided. The inputs for each case presented are also included as electronic file attachments available online with the thesis, among other easily downloadable data omitted from the results section which serves the reader better in an Excel sheet format. This data attached includes all reference results in the thesis as well as more detailed, 1/11<sup>th</sup> axial pin division fission density values and uncertainties for each full core and single assembly benchmark.

## CHAPTER 1. INTRODUCTION

The Small Modular Advanced High-Temperature Reactor (SmaHTR) is a Fluoride-salt-cooled High Temperature Reactor (FHR) Small Modular Reactor (SMR) detailed by Oak Ridge National Laboratory in their 2010 report.<sup>1</sup> The SmaHTR design is a thermal spectrum reactor fueled by Low-Enriched Uranium (LEU) in the form of tri-isotropic (TRISO) particle-graphite compacts. The ORNL report details three fuel-shape variants of the preconceptual design, but this thesis only details stylized designs based on the cylindrical pin-type fuel preconceptual design. Henceforth, the cylindrical pin design described in the ORNL report will be referred to as the “preconceptual SmaHTR design”.

As advanced reactor technologies are explored further, the verification and validation remain a challenge for neutronics tools. Thus, it is necessary to create benchmarks featuring these advanced reactor technologies. The molten salt coolant, small core size, and highly heterogeneous fuel compacts make this a unique problem of interest for testing neutronics methods. In creating this stylized set of reference problems, the lack of reactivity control mechanisms in the preconceptual design as well as the significant coolant bypass flow were significant gaps that had to be addressed first. Additionally, some simplifications were made to the benchmark problem as some support structures are not detailed for the design. The simplifications performed to create the stylized design have a small impact on the physics of the problems and therefore not important for benchmarking computation methods and code. The stylized designs this thesis details which feature the above simplifications and addressed gaps will be referred to as the “stylized design” and/or “stylized benchmark” henceforth. Preliminary work has been published to provide results

for a two-dimensional (2-D) stylized benchmark based on the SmAHTR in controlled, uncontrolled, and critical cases.<sup>3</sup>

It is believed this set of benchmark problems will function as excellent additions to the previously published FHR benchmark problems<sup>4</sup> for numerical benchmarking of neutronic tools for analysis of FHRs, due largely in part to the unique characteristics of this SMR FHR design.

## **CHAPTER 2. SUMMARY OF ORNL PRECONCEPTUAL DESIGN SPECIFICATIONS**

The preconceptual design report for the SmAHTR specifies three concentric rings of hexagonal assemblies surrounded by a radial graphite reflector for the core. In the pin-type-fuel design, each assembly contains solid cylindrical fuel pins and cylindrical moderating pins arranged in a hexagonal lattice. Each fuel pin is a graphite-cladded, graphite and TRISO compact with 50% volumetric packing fraction (VPF). This packing fraction provides a total core loading of 1556.4 kg uranium (19.75 wt%  $^{235}\text{U}$ ), which was used in the preconceptual report to provide a fresh core excess reactivity of 269.4-mk and core lifetime of 3.52 years.<sup>1</sup> The moderating pins are cylindrical pins of pure graphite. In the core there are no support structures specified, and both fuel and moderating pins are uniform axially throughout the 4-meter height of the core. Neither control rods nor burnable poison are specified for the design. The geometry and material composition that yields this loading and lifetime for the original design are detailed below.

### **2.1 Radial Layout**

The radial layout for the preconceptual design is depicted in Figure 1 below. The preconceptual design is composed of 19 hexagonal assemblies arranged in three concentric rings and surrounded by graphite reflector bounded at a 1.5-m radius from the center of the core. Each assembly is identical in arrangement and composition, with the same hexagonal lattice of fuel pins and graphite moderating. The hexagonal assemblies are arranged at a 45-cm pitch, and the reflector surrounding the 19 assemblies features eighteen, 6-cm radius coolant channels. The holes are assumed to be centered at a 45-cm pitch from third row of assemblies. Outside of the reflector, 25-cm of FLiBe surrounds the core. The FLiBe

coolant is composed of a 2:1  ${}^7\text{LiF}$  to  $\text{BeF}_2$  ratio, with lithium enriched to 99.995%  ${}^7\text{Li}$  to simulate nearly pure  ${}^7\text{Li}$ . The molten salt is contained within a 2.5-cm thick Hastelloy-N reactor vessel wall.

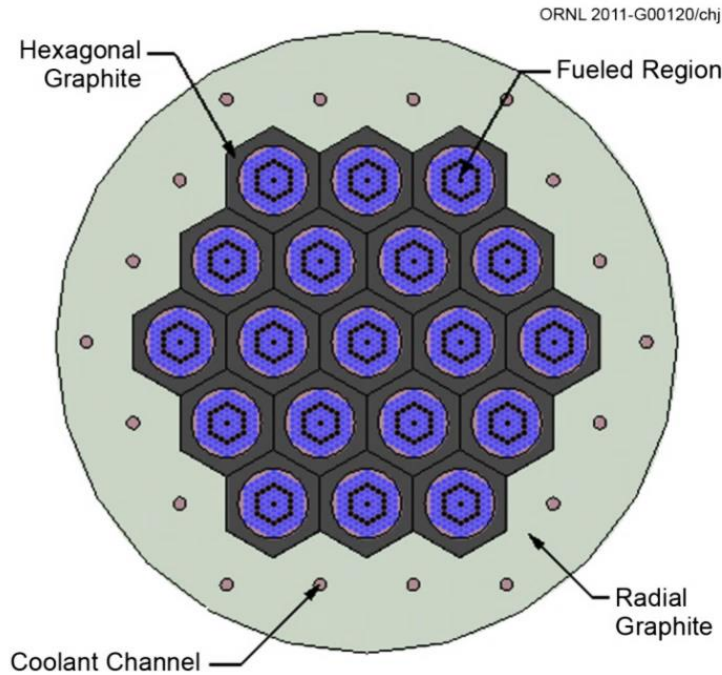


**Figure 1. Original SmaHTR Core Cross Section<sup>1</sup>**

## 2.2 Axial Layout

Each assembly is axially uniform, as no followers, support structures, or layers are specified within the 4-m tall core. The 9-m tall vessel includes the top closure flange, heat exchangers, reflector, and core. The heat exchangers, flow skirting, and core bonnet are depicted in the report without fully specified dimensions for the pin type design. Some dimensions for structural components are provided for the plank-type fuel design in the ORNL report, but do not necessarily apply for the pin-type fuel. Figure 2 below presents the relevant axial schematics for the cylindrical pin-type fuel preconceptual design.

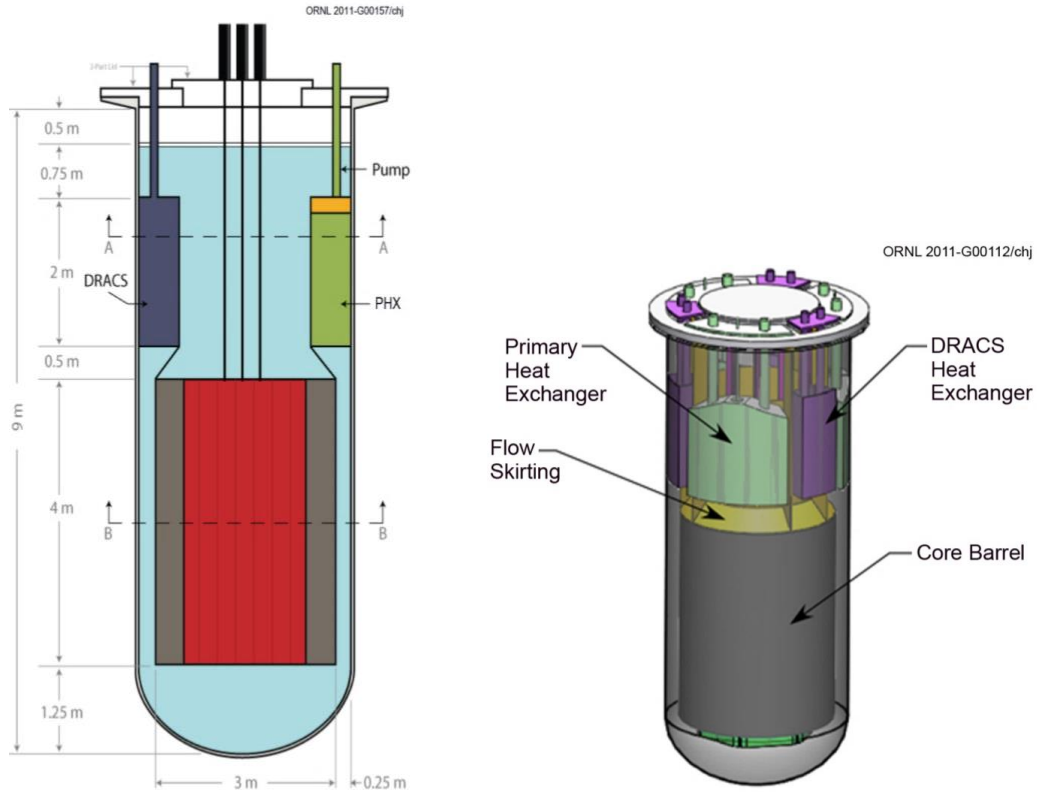


**Figure 2. SmAHTR Axial Schematic from ORNL Report<sup>1</sup>**

The graphite reflector which surrounds the core is described as five, 80-cm fuel block layers. Below the core, there is a rounded vessel wall of 1.25-m radius that contains FLiBe. The DRACS (Direct Reactor Auxiliary Cooling System) and PHX (Primary Heat Exchanger) are depicted above the core, but material properties and geometric specifications are not included.

### 2.3 Assembly Specifications

The assembly consists of fuel and moderator pins in a hexagonal lattice, a cylindrical coolant channel, and an outer hexagonal boundary. The six concentric rings of fuel and moderator pins in the hexagonal lattice have a pitch of 3.08-cm. The center pin and middle ring of pins make up the 19 graphite pins of 1.4-cm radius. The remaining 72 pins are 1.1-

cm radius graphite-TRISO compacts at 50% VPF, clad with a 3-mm thick graphite layer to yield an outer radius of 1.4-cm. The cylindrical coolant channel within the assembly has a 16.94-cm radius opening, and the outer hexagonal boundary has an apothem of 22.5-cm. The assembly in the original preconceptual design from the ORNL report<sup>1</sup> is shown below in Figure 3. Within the assembly, spacers for the cylindrical pin fuel type are not specified, nor are any other support structures to suspend the pins either within, above, or below the core.

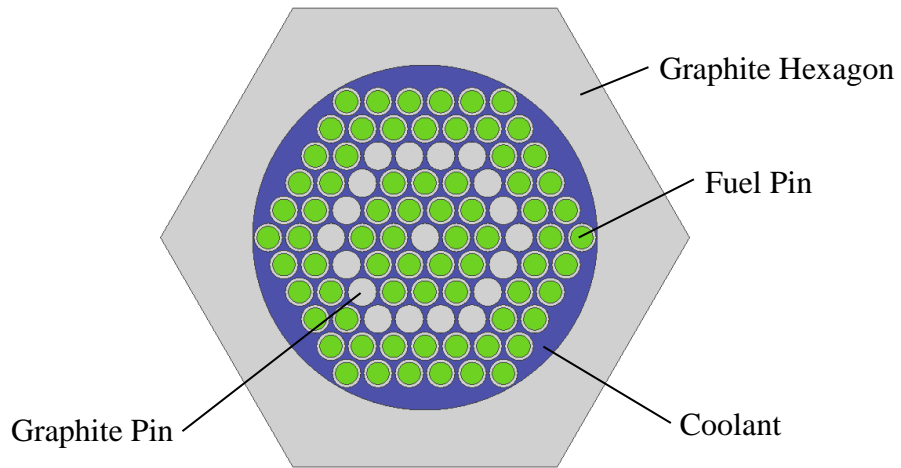


**Figure 3. SmAHTR Cylindrical Fuel Pin Assembly**

## **2.4 Fuel Composition**

The TRISO fuel particles are packed in the graphite at a 50% volumetric packing fraction. The same TRISO particles tested in the Advanced Gas Reactor TRISO irradiation experiment-1 (AGR-1) are referenced in the ORNL report as a potential choice for the cylindrical fuel compacts. To achieve the 1556.4-kg uranium core loading at 50% VPF however, a larger UCO kernel than what was specified for the AGR-1 must be used (such as that of the AGR-2). The larger  $UC_{0.5}O_{1.5}$  kernel diameter of the TRISO from the AGR-

2 experiment at 50% VPF provides the specified loading and packing fraction. Henceforth, TRISO parameters referenced in the report are those of the AGR-2 experiment.

## CHAPTER 3. STYLIZED BENCHMARK SPECIFICATIONS

In creating the stylized benchmark problem, the gaps remaining from the preconceptual design in addition to thermal hydraulic considerations were addressed first. Simplifications and assumptions about the geometry of the reactor were then made in addition to the necessary modifications, as a prohibitively complex problem is not ideal for benchmarking computational tools. The stylized design preserves the complexity resulting from the highly heterogeneous fuel. All modifications to the preconceptual design are discussed below, and the fully detailed stylized problem is presented. We note that these modifications were made to fill gaps, but none were necessarily optimized for design purposes as this was outside of the scope of the intended work for this paper.

### 3.1 Coolant Channel Modifications

Related work on the steady-state thermal hydraulic model for the stylized design was performed by S. Chandrasekaran and S. Garimella and detailed in their 2020 *Nuclear Technology* paper, “Steady-State Thermal-Hydraulic Model for Fluoride-Salt-Cooled Small Modular High-Temperature Reactors,” finding that the amount of bypass flow in the original design was significant, so modifications to the preconceptual design which would allow a thermal hydraulics model to function properly were essential.<sup>5</sup> The shape of the coolant channel in the assembly was modified from a cylinder of 16.94-cm radius to a hexagonal channel of equivalent flow area with a 16.132-cm apothem. Additionally, the distance between the outer row of pins and the wall of the assembly coolant channel was reduced by increasing the pin pitch from 3.08-cm to 3.29-cm to redistribute the pins and create an even gap spacing between pins and the walls. These modifications significantly

reduce the bypass flow in the reactor. While altering the geometry impacts the fission density distribution in the assembly, the amount of coolant and graphite surrounding the pins are preserved in this alteration, thus minimizing any impact on the neutronics of the problem. Figure 4 below shows the assembly before and after the modifications, with FLiBe indicated in blue, graphite in grey, and fuel rods in green.

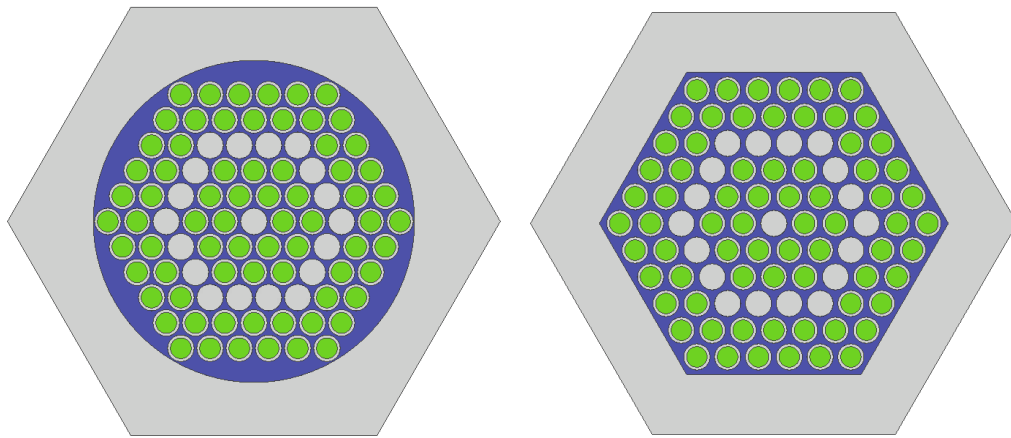


**Figure 4. Original Assembly (Left) and Modified Assembly (Right)**

### **3.2 Burnable Poison Content**

The preconceptual design report only made suggestions, but it did not specify definitively any burnable poison to be included in the reactor system, so graphite compacts of coated particles containing boron were included for burnable poison. Similarities between this pin type design and the Very High Temperature Reactor (VHTR)<sup>6</sup> design (e.g., TRISO, pin type fuel, and graphite matrix) drove the decision to utilize the coated boron particles in the stylized SmAHTR benchmark set. The BP are dispersed in 6 graphite pins, each located in the corners of every assembly. These graphite pins containing BP particles replace pins designated as fuel in the preconceptual design, and this has the

significant effect of reducing the total core loading by nearly eight percent. The particles are the same as those specified in the VHTR design: 200-micron diameter nat. boron (19.9%  $^{10}\text{B}$  and 80.1%  $^{11}\text{B}$ ) carbide kernels coating with an 18-micron thick carbon buffer layer and a 23-micron thick pyrolytic carbon outer layer.<sup>6</sup> The particles are centered within a rectangular lattice structure of 0.06982-cm side lengths and height of 0.07984-cm height. The infinite lattice VPF differs from the true modeled VPF in the stylized design. In an infinite medium, these lattice dimensions provide a VPF of 3.03%, but in the stylized design, the lattice is cut by the cylindrical pin boundaries, yielding a true VPF for the stylized design of 2.99%. It is also important to note that the lattice for each burnable poison pin is centered axially and radially within each pin. The considerations associated with the infinite lattice modeling of particles is discussed further in the section on TRISO, where the VPF is much higher. The BP-containing pins are the same dimension as the fuel pins: 1.1-cm radius clad in 0.3-cm thick graphite to maintain the same gap spacing between pins. Figure 5 below shows the stylized assembly before and after the addition of burnable poison pins. The burnable poison pins in Figure 5 are indicated with pink.

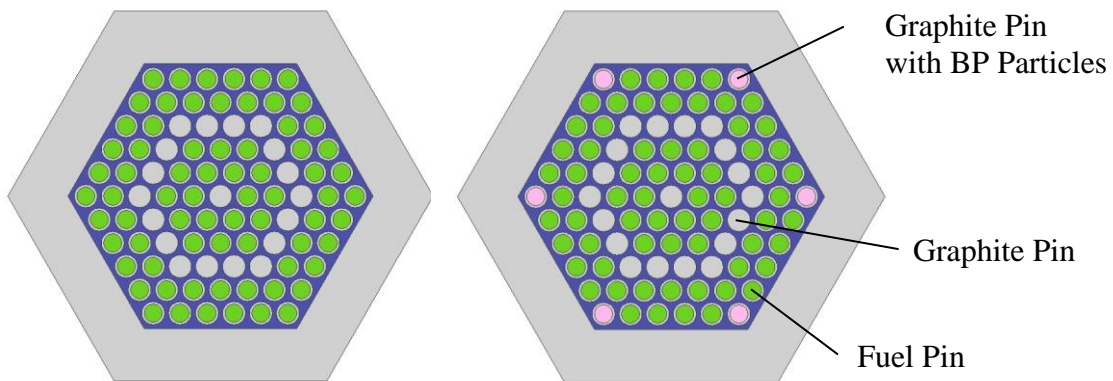


**Figure 5. Stylized Assembly Before (Left) and After Addition of Burnable Poison Rods (Right)**

### 3.3 Control Rods

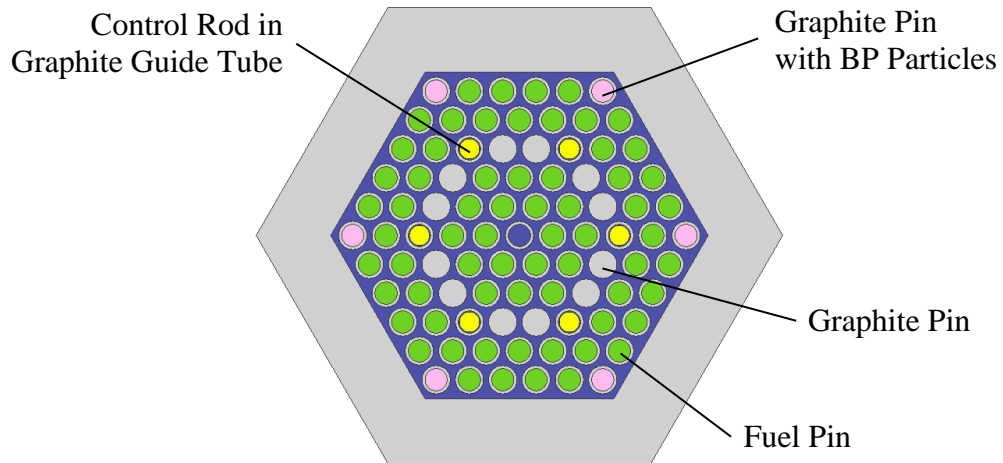
To manage reactivity and provide an avenue for power shaping, control rods are added to the assembly. The preconceptual report mentioned the possibility of control rods in the pin-type design, but it did not designate a location or definitively provide a material. However, the report considered using boron for control purposes, so for the stylized design, boron carbide rods are utilized for the active control mechanisms. Three modifications are considered and modelled for the stylized design, referred to as either control rod placement or design A, B, or C below. In each of the three designs, rods of borated graphite are specified for each assembly in a 55:1 carbon to boron-carbide ( $B_4C$ ) ratio, using a natural enrichment of boron (19.90%  $^{10}B$ ). This is equivalent to a 14:1 carbon to boron ratio, and is specified that way in the material summary provided in Table II below provides material properties with their atomic composition, density, and modeled temperature below. It should be noted that these compositions are all in atomic fractions, and each material except for the control rod boron carbide is already normalized to sum to one.

Table II below. The control rods are designated as 1.0-cm radius pins with a 0.1-cm gap and 0.3-cm thick guide tube for coolant to flow through in each case. No control rod followers or support mechanisms are specified with control rods. Neither the locations nor the material composition of these rods are considered to be optimized, but they are included with different options since they are essential in closing the gaps left by the preconceptual design and achieving a critical core. Control rod placement A and B both implement 6

control rods in each assembly. In design A, the control rods are located within the coolant channel and replace six graphite moderating pins. Design B instead specifies control rods in the outer hexagonal graphite region of the assembly, and it does not alter any moderating pins. Design C is similar to B, but it considers only three control rods in the hexagonal graphite of the assembly instead of six.

### *3.3.1 Control Rod Placement A*

Control rod placement A substitutes in six control rods where graphite moderating pins were located in each assembly. Each of the six corners of the middle row of the assembly which were previously 1.4-cm radius graphite pins were substituted with 1.0-cm radius control rods with a 0.1-cm gap surrounded by a 0.3-cm thick graphite guide tube which yields a 1.4-cm outer radius. The 0.1-cm gap between the control rod and guide tube is filled with FLiBe, and the 1.4-cm outer radius of the guide tube maintains the same pitch between other fuel and moderating pins in the assembly. A single, graphite guide tube is included in place of the center moderating pin for instrumentation, but it only contains FLiBe in all configurations. When control rods are withdrawn from the assembly, the guide tubes are filled with FLiBe. Figure 6 below illustrates the six control rod placements and central guide tube. The control rods in the corners of the middle ring are indicated with yellow.



**Figure 6. Control Rod Placement A**

### 3.3.2 Control Rod Placement B

Control rod placement B features the six control rods arranged in the outer graphite region of the fuel assembly. Each of the six 1.0-cm radius control rods are inserted in 1.1-cm radius holes within the hexagonal graphite, equidistant from the inner and outer hexagonal boundaries in the center of each face of the hexagonal graphite. When control rods are uninserted in this design, FLiBe fills the 1.1-cm radius holes in the hexagonal graphite. Figure 7 below shows the cross-sectional view of the assembly with the six rods in the hexagonal graphite region.

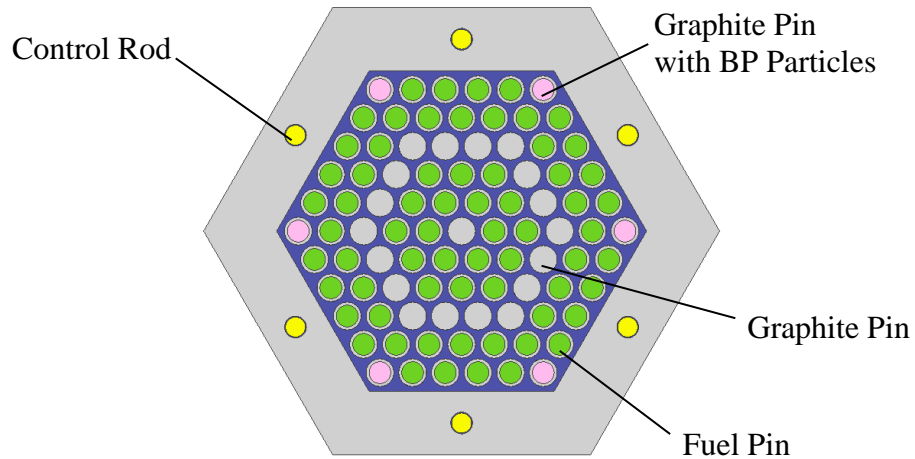


**Figure 7. Control Rod Placement B**

### 3.3.3 Control Rod Placement C

Control rod placement C includes only three control rods of 1.0-cm radius in the outer graphite region of the assembly. Each rod is situated in a 1.1-cm radius hole where FLiBe fills the 0.1-cm gap between the control rod and the graphite. The holes for the control rods exist on alternating sides of the hexagonal prism, equidistant from the inner and outer boundaries of the hexagonal graphite. The intention of this control rod option was to create a single assembly design that when assembled for the full core stylized problem, would place a single control rod between each assembly opening as opposed to the two present between each assembly for a full core using assembly B. Figure 8 below shows the assembly cross section for placement C.

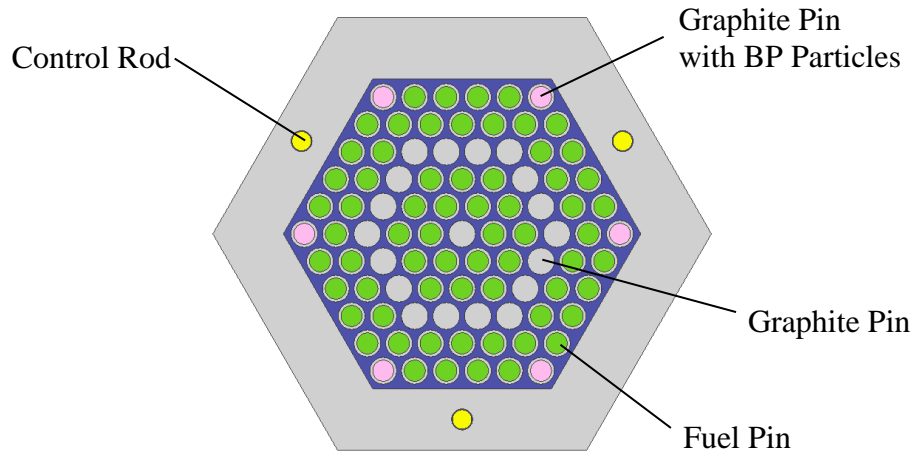


**Figure 8. Control Rod Placement C**

### 3.4 TRISO Fuel

The TRISO material properties and dimensions follow from the AGR-2 experiments which feature specifications similar to AGR-1 but have the larger kernel size necessary to achieve the desired core loading and packing fraction. The geometry, material, and density of each TRISO layer is based on the AGR-2 TRISO, and those specifications are summarized in Figure 9 below.<sup>7</sup>

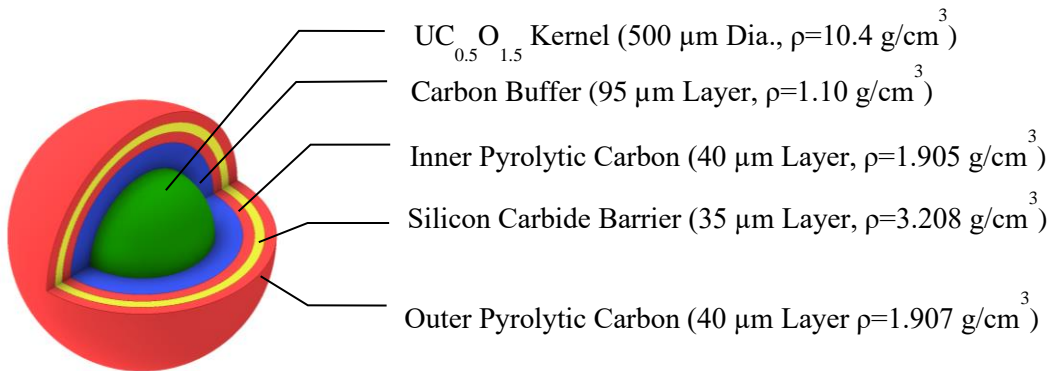


**Figure 9. TRISO Composition**

The TRISO particles are modeled in full heterogeneity in a uniformly-filled infinite hexagonal lattice cut by the boundaries of the 1.1-cm radius pin. The hexagonal lattice has the following dimensions: a 0.0491-cm apothem and 0.09324-cm height. In an infinite medium, this lattice provides a VPF of 52.36%, but in the stylized design, the VPF is reduced to 50.43% due to the lattice being cut by the boundaries of the cylindrical pin. The 50.43% VPF is exact VPF in the stylized design which yields the results below. This type of modeling is unrealistic for TRISO-packed graphite, as the particles have a non-random distribution and are cut by pin cell boundaries, but it provides the nearly 50% packing fraction detailed in the preconceptual report. The most accurate representation of the TRISO would be to model each TRISO at randomized positions which do not clip the boundaries of the pin while still achieving nearly 50% VPF, but the impact this has on the computational efficiency of the design can be prohibitive. Solely the utilization of an infinite hexagonal lattice over an ordered lattice which prevents TRISO from intersecting the pin boundaries proved far more computationally efficient in achieving low-uncertainty results. When using lattices, MCNP5 can utilize a built-in feature designed to add a limited degree of randomness to lattice-packed particles called by the URAN card, but this card was not included in the input file as it has no practical use for particles with nearly a 50% packing fraction. The URAN card operates by slightly shifting the particles a random amount within their lattice structure to create a stochastic geometry distribution,<sup>2</sup> but the high packing fraction of this design renders this feature to a near-negligible impact on the core. This MCNP5 feature has been proposed to not just provide a more realistic random structure, but more importantly to reduce the uncertainty present from variation in the fuel mass and distribution resulting from minute differences in the fuel lattice center (origin).

This effect was investigated for TRISO in a High Temperature Engineering Test Reactor (HTTR) fuel block in work done by Dan Ilas and Jess Gehin and presented in their PHYSOR 2010 conference proceeding, “HTTR Fuel Block Simulations with SCALE”.<sup>8</sup> The results of their investigation of this effect with MCNP5 for their HTTR fuel block yielded up to 2% variations in the total fuel mass for the annular fuel pin analyzed. It is an important consideration to note in creating a stylized design, and the VPF stated in this thesis for the TRISO and BP take this into account. Despite the drawbacks to the structured lattice approach, the uniformly distributed, infinite hexagonal lattice of TRISO still maintains the high heterogeneity and VPF essential to the complexity of this stylized benchmark problem set.

### **3.5 Stylized Core Specifications**

The stylized core and assembly are presented below for control rod placement A. Notes are provided about dimensions which change for options B and C.

#### *3.5.1 Stylized Radial Layout*

The stylized benchmark core problem has 19 identical assemblies arranged with a 45-cm pitch to form three rings of assemblies for the reactor core. Each assembly has the same arrangement of fuel pins, graphite pins, burnable poison pins, and control rod locations. The core is surrounded by a graphite reflector with eighteen 6-cm radius openings for coolant to flow through, also centered at a 45-cm pitch from the outer ring of assemblies. The graphite reflector fills all area between the outer assembly ring and the 150-cm radius core boundary. Figure 10 below presents the cross-sectional view of the

modified stylized reactor core for control rod option A. In the radial direction, the 150-cm radius graphite reflector is considered the external boundary of the problem.

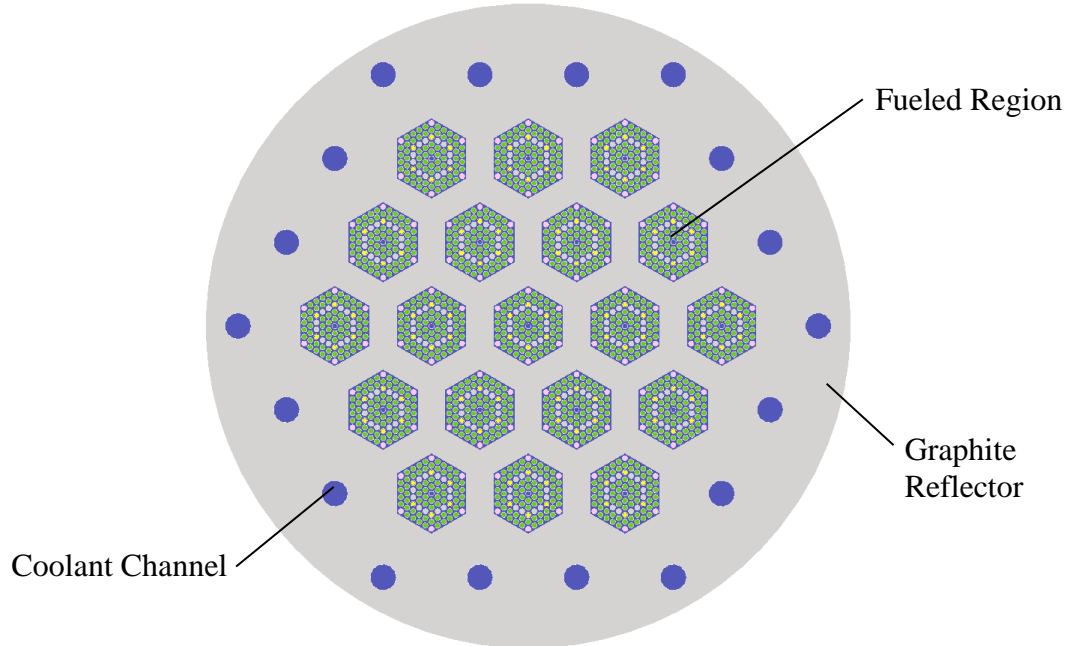


**Figure 10. Stylized SmAHTR Core Cross Section for Control Rod Placement A.**

### 3.5.2 Stylized Axial Layout

In the axial direction, the core itself remains uniform except for control rods, which may be inserted partially into the core. The critical configuration detailed later for control rod placement B features partially inserted rods which protrude into the coolant above the core. Each assembly features the pins and control rods without support structures or followers, as simple control rods were included in the stylized design solely to address gaps in the preconceptual report necessary for this benchmark set. Above the core, the heat exchangers are not modeled since their composition is largely unknown and not neutronically significant for this stylized benchmark. Instead, a cylindrical layer of FLiBe

50-cm thick is modeled above the core. Likewise, a 50-cm layer of FLiBe is modeled below the core. When control rods are fully inserted, there is no control material that extends into the FLiBe above or below the core, nor when control rods are fully withdrawn. Exact geometric and material specifications for each full core and single assembly case are detailed below.

### *3.5.3 Geometric and Material Specifications*

Three assembly configurations are considered in the problem sets: uncontrolled, controlled, and partially controlled. In the uncontrolled case, all control rods are withdrawn fully, leaving FLiBe to fill the control rod guide tubes in the assembly. In the controlled case, all control rods are inserted fully, with FLiBe filling the gap between the rods and guide tubes/channels. In the partially controlled case, control rods are inserted from above into the assembly as a cluster. In this case, the area below the control rods is filled by FLiBe, and the partially inserted 400-cm tall control rods extend into the FLiBe above the assembly. Axially, the 400-cm tall assembly is divided into eleven, 36.36-cm slices to provide axial data for the benchmark problem. In the uncontrolled and controlled full core cases, the 19 assemblies are all either fully withdrawn or fully inserted, respectively with 50-cm of FLiBe modeled above and below the core. In the near-critical full core cases, the 19 assemblies are a mixture of controlled, uncontrolled, and partially controlled assemblies, where control rods extend into the FLiBe above the core where partially controlled assemblies exist. A summary of the geometric specifications for these cases are detailed in Table I below.

**Table I. Geometric Specifications**

<b>Components</b>	<b>Dimension</b>
Assembly <ul style="list-style-type: none"> <li>- Outer Hexagonal Graphite Apothem</li> <li>- Inner Hexagonal Graphite Apothem</li> <li>- Pin Pitch</li> <li>- Height</li> <li>- FLiBe Thickness Above Assembly</li> <li>- FLiBe Thickness Below Assembly</li> </ul>	22.500-cm 16.132-cm 3.290-cm 400.000-cm 50.000-cm 50.000-cm
Fuel Pin <ul style="list-style-type: none"> <li>- Radius</li> <li>- Cladding Thickness</li> </ul>	1.100-cm 0.300-cm
Graphite Pin <ul style="list-style-type: none"> <li>- Radius</li> </ul>	1.400-cm
Burnable Poison Pin <ul style="list-style-type: none"> <li>- Radius</li> <li>- Cladding Thickness</li> </ul>	1.100-cm 0.300-cm
Control Rod: Placement A <ul style="list-style-type: none"> <li>- Radius</li> <li>- Gap Thickness</li> <li>- Guide Tube Thickness</li> </ul>	1.000-cm 0.100-cm 0.300-cm
Control Rod: Placement B and C <ul style="list-style-type: none"> <li>- Radius</li> <li>- Gap Thickness</li> </ul>	1.000-cm 0.100-cm
Core Reflector & Coolant (Full Core Cases) <ul style="list-style-type: none"> <li>- Reflector Coolant Channel Pitch</li> <li>- Reflector Coolant Channel Radius</li> <li>- Outer Reflector Radius</li> </ul>	45.000-cm 6.000-cm 150.000-cm

Table II below provides material properties with their atomic composition, density, and modeled temperature below. It should be noted that these compositions are all in atomic fractions, and each material except for the control rod boron carbide is already normalized to sum to one.

**Table II. Material Specifications**

Components	Isotope, Atomic Composition	Density (g/cc)	Temp (K)
Control Rod – Boron Carbide	<sup>10</sup> B, 0.1990 <sup>11</sup> B, 0.8010 C, 14.0000	2.266	800
BP, Fuel, Moderator – Graphite Matrix Control Rod – Graphite Guide Tube	C, 1.0000	2.266	800
All Pins – Graphite Cladding	C, 1.0000	2.266	800
BP – Boron Kernel	<sup>10</sup> B, 0.1990 <sup>11</sup> B, 0.8010 C, 0.2500	2.470	1200
BP – Carbon Buffer	C, 1.0000	1.000	1200
BP – Pyrolytic Carbon (PyC) Layer	C, 1.0000	1.870	1200
Coolant – FLiBe	<sup>6</sup> Li, 0.0001 <sup>7</sup> Li, 1.9999 <sup>9</sup> Be, 1.0000 <sup>19</sup> F, 4.0000	1.940	900
TRISO – UC <sub>0.5</sub> O <sub>1.5</sub> Kernel	<sup>235</sup> U, 0.06650 <sup>238</sup> U, 0.26683 C, 0.16667 <sup>16</sup> O, 0.50000	10.400	1200
TRISO – Carbon Buffer	C, 1.0000	1.100	1200
TRISO – Inner PyC	C, 1.0000	1.905	1200
TRISO – Outer PyC	C, 1.0000	1.907	1200
TRISO – Silicon Carbide	C, 0.50000 <sup>28</sup> Si, 0.461485 <sup>29</sup> Si, 0.023416 <sup>30</sup> Si, 0.015436	3.208	1200

It should also be noted that the continuous energy nuclear data libraries utilized to obtain the results for this stylized benchmark set come from the Evaluated Nuclear Data Files ENDF/B-VII.0 release. The exact data library extensions for each material are provided in the input file documentation attached online with this thesis. The ENDF/B-VII.0 thermal S( $\alpha,\beta$ ) cross-section libraries are called in the input files for all instances of graphite.

## **CHAPTER 4. BENCHMARK RESULTS**

Results are presented below for the 3-D full core and single assembly cases below. The necessary details (i.e., boundary conditions, criticality code specifications) required for attaining the results for each case are described in their respective section below. The full geometry for the single assembly and full core cases for each control rod placement option are detailed above in CHAPTER 3.

### **4.1 Results Summary**

The benchmark results were calculated for the different cases and control rod placements using the continuous energy code MCNP5.<sup>2</sup> Input decks for all cases are provided as supplemental files to the thesis, as their inclusion in the appendices would not be feasible due to the large number of files and individual file length. For the benchmark results, the boundary conditions for full core cases are vacuum at all external surfaces, and the boundary conditions used for the full-length single assembly calculations are as follows: full specular reflection at the radial boundaries and vacuum at the top and bottom surfaces. The full-length single assembly was modeled for uncontrolled and controlled cases in each of the three control rod placement designs. The stylized cores were evaluated for an uncontrolled case, a controlled case, and a near-critical case for control rod placement A and B, but in only controlled and uncontrolled cases for control rod placement C. The near critical case for placement A features full control rod withdrawal in every other outer row assembly and full control rod insertion in all other locations as highlighted in Figure 11 below. The near-critical configuration for control rod placement B features a

mixture of fully withdrawn, fully inserted, and partially inserted control rod “bundles” as depicted in Figure 12 below.

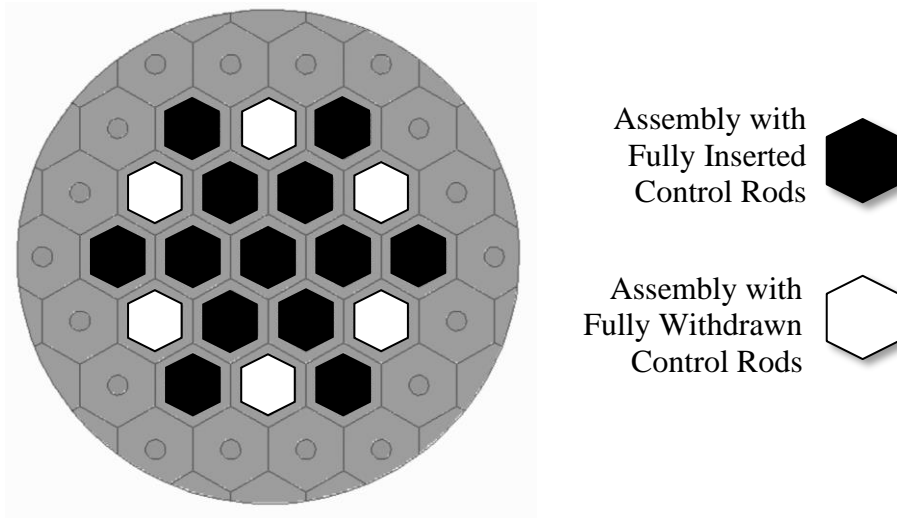


**Figure 11. Control Rod Pattern for Near-Critical Core – Control Rod Option A**

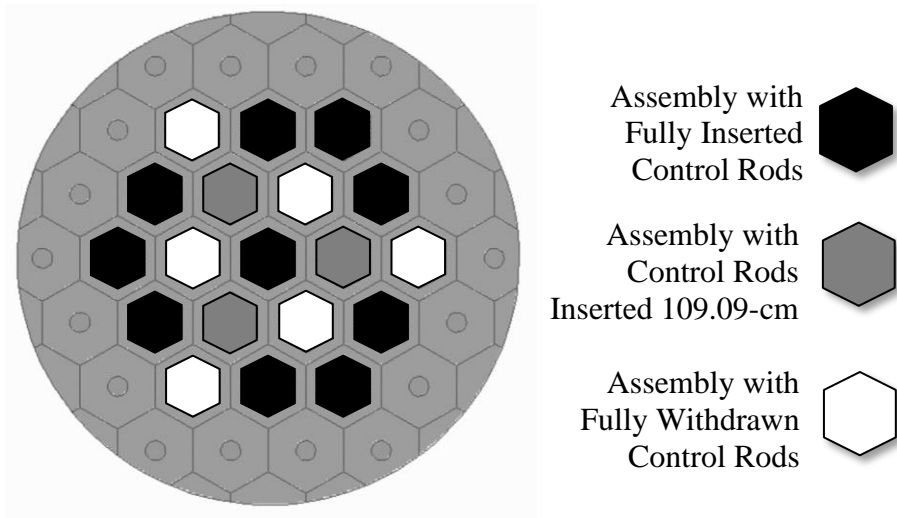


**Figure 12. Control Rod Pattern for Near-Critical Core – Control Rod Option B**

The benchmark results for the different cases are organized below in Table III. The results below were calculated in the single assembly cases with the following criticality code parameters: 60,000 particles per cycle, 100 skipped cycles, 800 active cycles, and an initial  $k_{eff}$  estimate of 1.00. In the full core cases, the following criticality parameters were:

60,000 particles per cycle, 300 skipped cycles, 5000 active cycles, and an initial  $k_{eff}$  estimate of 1.00. These parameters were chosen to provide low statistical uncertainty in the benchmark results and ensure all statistical tests for convergence were met. The warnings that appear when running the inputs for these cases are harmless and expected warnings for geometric surface redundancy or notifications that the same material is called for at different temperatures and densities.

**Table III. Comparison of Stylized Benchmark Criticality Results**

Problem Type	Configuration	$k_{eff}$ and 1-Sigma Uncertainty		
		Placement A	Placement B	Placement C
Single Assembly	Uncontrolled	$1.22994 \pm 4$ pcm	$1.23038 \pm 4$ pcm	$1.23207 \pm 4$ pcm
Single Assembly	Controlled	$0.97883 \pm 4$ pcm	$0.89248 \pm 4$ pcm	$1.04953 \pm 4$ pcm
Full Core	Uncontrolled	$1.15694 \pm 5$ pcm	$1.15786 \pm 5$ pcm	$1.15940 \pm 5$ pcm
Full Core	Controlled	$0.92556 \pm 5$ pcm	$0.84352 \pm 5$ pcm	$0.97200 \pm 5$ pcm
Full Core	Near-Critical	$0.99312 \pm 5$ pcm	$0.99993 \pm 5$ pcm	N/A

Table III above presents a summary of these results for the full core and single assembly cases, and the radial fission density distributions are provided for those cases below. Although not needed to interpret the results, Figure 13 below provides the numbering scheme for the pin indices, which is necessary when referencing the attached Excel files containing the complete 3-D pin fission density data, accessible with this



lieu of moderating material within the hexagonal graphite. Uncontrolled assembly B only has slightly more moderating material than A due to the center pin of assembly A having an empty guide tube which removes moderating material from the design when compared to the preconceptual design. These differences are nearly indistinguishable on the uncontrolled radial fission density distribution heat maps of Figure 14, Figure 15, and Figure 16, but it is evident from their differing uncontrolled k-effective results presented in Table III which reflect an increasing trend for the uncontrolled  $k_{\text{eff}}$  as predicted from assembly A to B to C. It is important to note that the results plotted in Figure 14 - Figure 16 are all plotted to the same color scale for proper comparison. The 1-sigma uncertainties range from a minimum of 0.0281% to a maximum of 0.0345%.

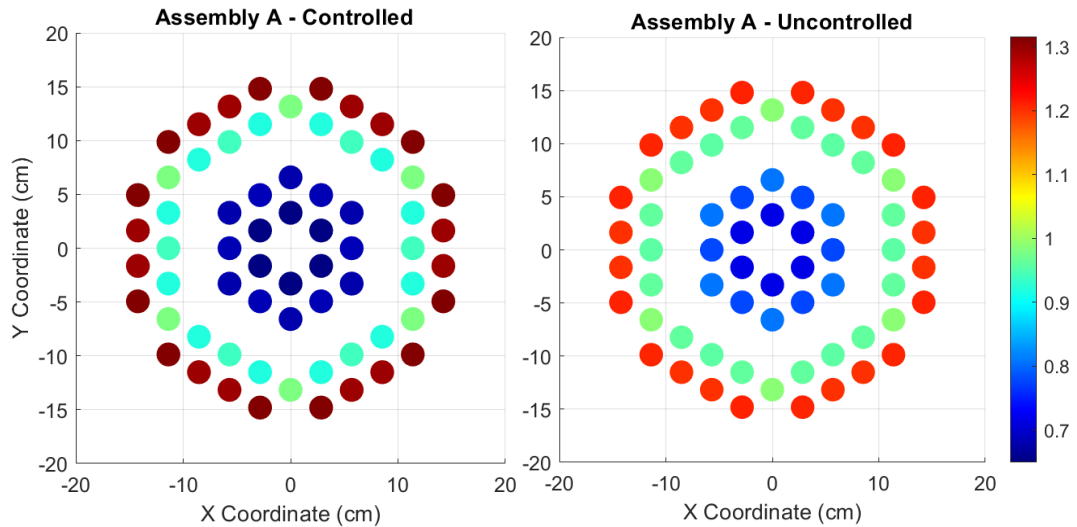


**Figure 14. Radial Fission Density Distribution for Controlled (Left) and Uncontrolled (Right) Assembly A**

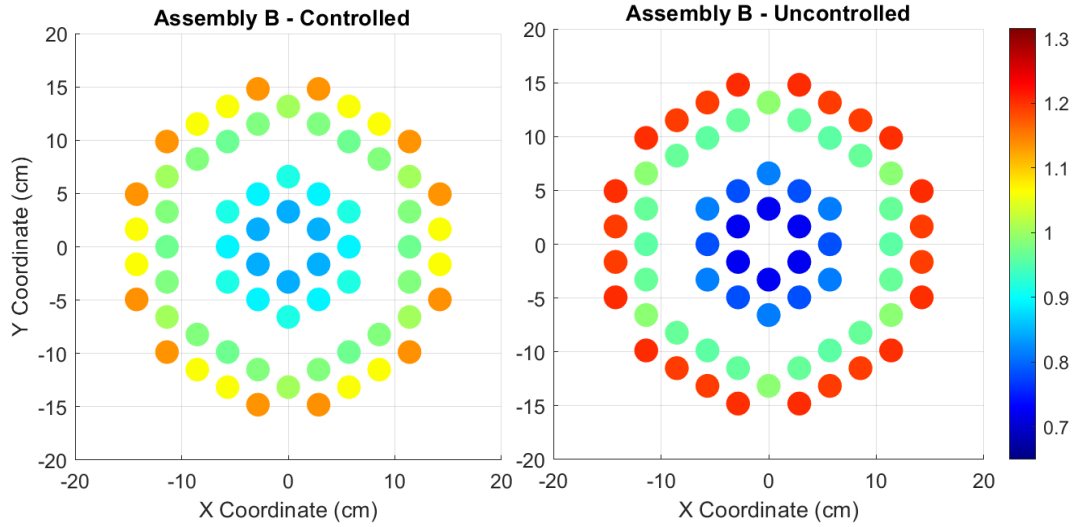


**Figure 15. Radial Fission Density Distribution for Controlled (Left) and Uncontrolled (Right) Assembly B**

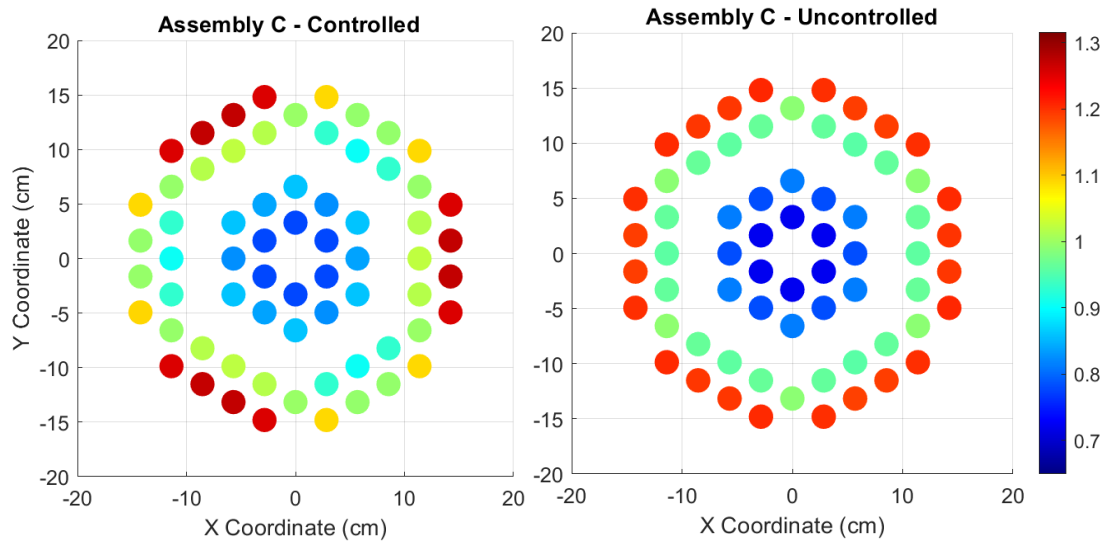


**Figure 16. Radial Fission Density Distribution for Controlled (Left) and Uncontrolled (Right) Assembly C**

There are significant differences in the radial fission density distributions across the controlled assemblies. Assembly A, which features control rods in the middle ring (the graphite and control rod ring) of assembly pins, is very cold within the graphite and control rod ring but significantly hotter outside it, as the two outermost rings of fuel pins are

heavily influenced by the amount of graphite in the outer hexagonal assembly graphite. Assembly B is considered an improvement upon design A, where the radial fission density distribution is noticeably flatter in the controlled case B than in A. By creating a design B where control rods are inserted into the hexagonal graphite, not only is the radial profile flattened, but the control rod worth is also increased. The difference in  $k_{\text{eff}}$  values from Table III between controlled designs A and B help illustrate this difference, as the controlled single assembly design B has a much lower  $k_{\text{eff}}$  than in the controlled single assembly design A ( $0.8925 \pm 4$  pcm and  $0.9788 \pm 4$  pcm for controlled single assembly B and A, respectively) despite having the same number of control rods in each. The controlled single assembly C yields radial fission density results still flatter than design A, but it was designed to work synergistically with other assemblies in the full core, as there would be alternating controlled sides such that the hot side of one assembly is against the cold side of another assembly.

The radial (axially-integrated) fission density distributions for the controlled and uncontrolled full cores A, B, and C are plotted in Figure 17, Figure 18, and Figure 19, respectively. A comparison of the near-critical cores A and B are provided in Figure 20 below. Figure 17 through Figure 20 are all plotted with the same color scale, so the color bar on the right side of each figure is consistent throughout each of the four figures. Across the four figures below, the relative uncertainty values range from a minimum of 0.1258% to a maximum of 0.2787%.

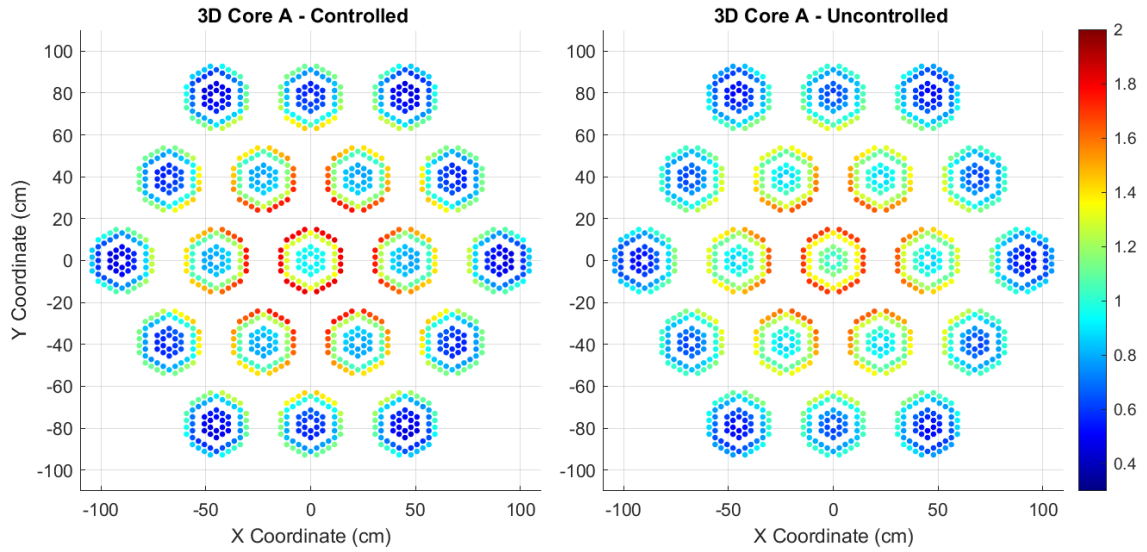


**Figure 17. Radial Fission Density Distribution for Controlled (Left) and Uncontrolled (Right) Core A**

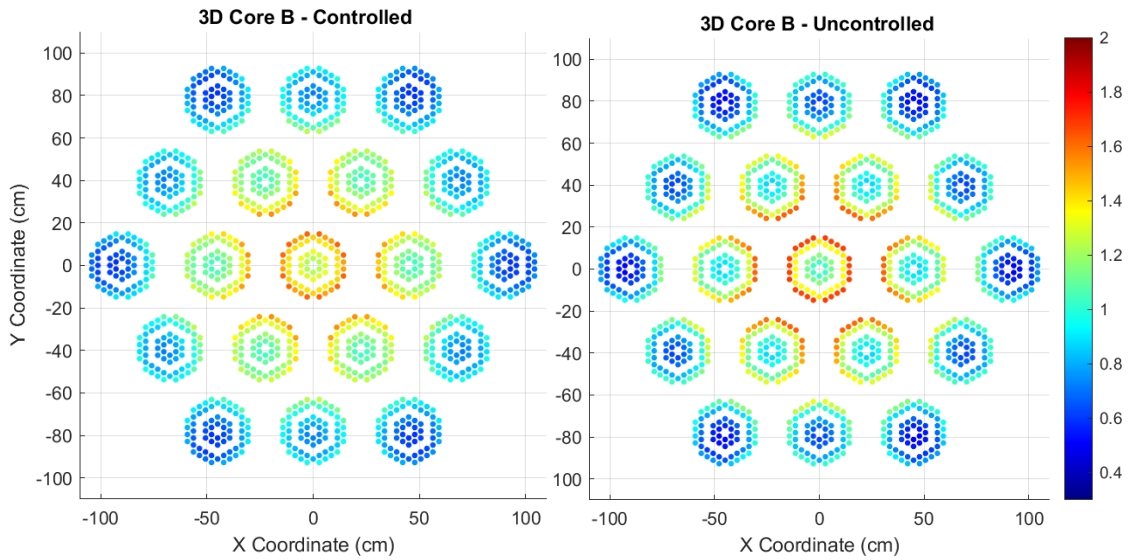


**Figure 18. Radial Fission Density Distribution for Controlled (Left) and Uncontrolled (Right) Core B**

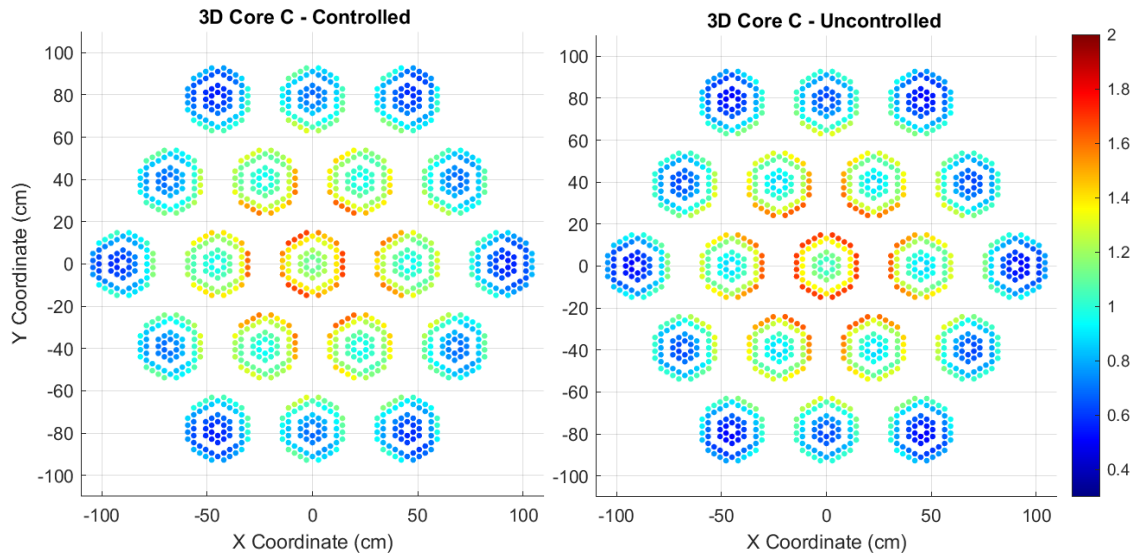


**Figure 19. Radial Fission Density Distribution for Controlled (Left) and Uncontrolled (Right) Core C**

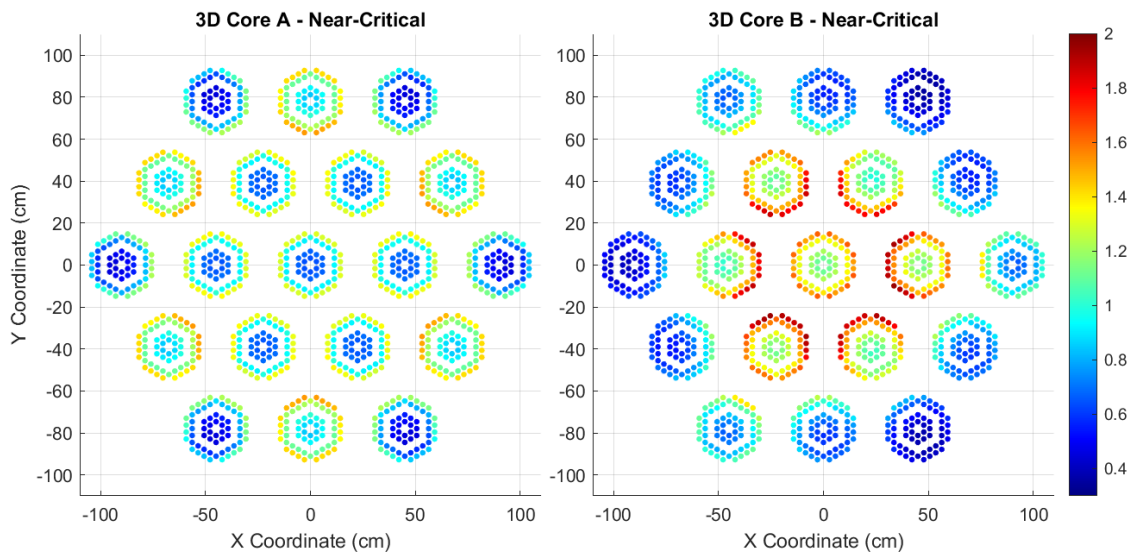


**Figure 20. Radial Fission Density Distribution for Near-Critical Core A (Left) and Near-Critical Core B (Right)**

There is no significant difference between the radial fission densities of the uncontrolled cores, similar to single assembly results. It reveals that in the uncontrolled cases, the radial fission density peaks in the center of the core, and is depressed in the outer

ring of assemblies, especially in the centers of the individual assemblies where the fuel is furthest away from the hexagonal graphite of each assembly. The controlled cases of cores B and C yield a flatter radial profile, which is in part due to the controlled core A featuring control rods inserted into the middle ring of each assembly, further depressing the already lower fission density areas whereas the control rods in cores B and C depress the higher flux graphite regions of each assembly.

Design A and B's near critical steady-state configurations were designed to yield a k-effective very close to one, as it is of significant benefit to have that case available for testing purposes. However, it should be noted that these cases were not necessarily optimized for parameters such as a flat power profile. For the loading patterns detailed in Figure 11 and Figure 12 above, the near-critical case for core A provides a relatively flat power profile in comparison to core B. Many loading patterns were tested, and the one provided above for core B yielded a k-effective closest to one, however it lacks the flattened profile core A features in its near-critical case.

### **4.3 Axial Fission Density Distribution Results**

The axial (radially-integrated) fission density distributions are plotted for the uncontrolled, controlled, and near-critical cases for cores with control rod placement A and B in Figure 21 and Figure 22, respectively. The axial fission density distribution is plotted for the uncontrolled and controlled cases for core C in Figure 23. Error bars are present on the axial plots below for the, but they appear as singular small horizontal lines for many data points because the relative uncertainties for the axial core layers is quite small. These values range from a minimum of 0.0131% to a maximum of 0.0450%.

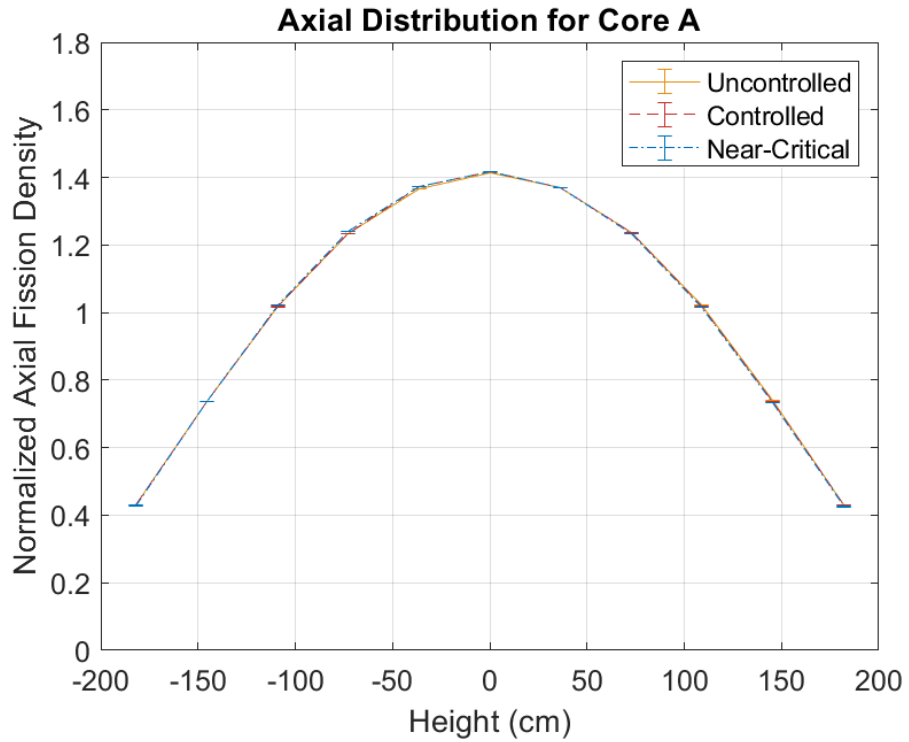


**Figure 21. Axial Fission Density Distribution for Core A**

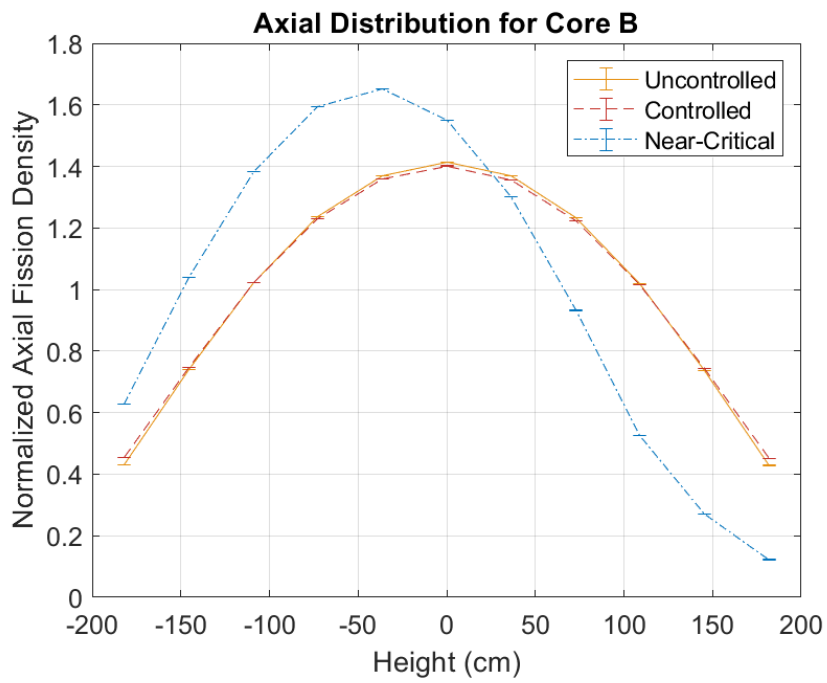


**Figure 22. Axial Fission Density Distribution for Core B**

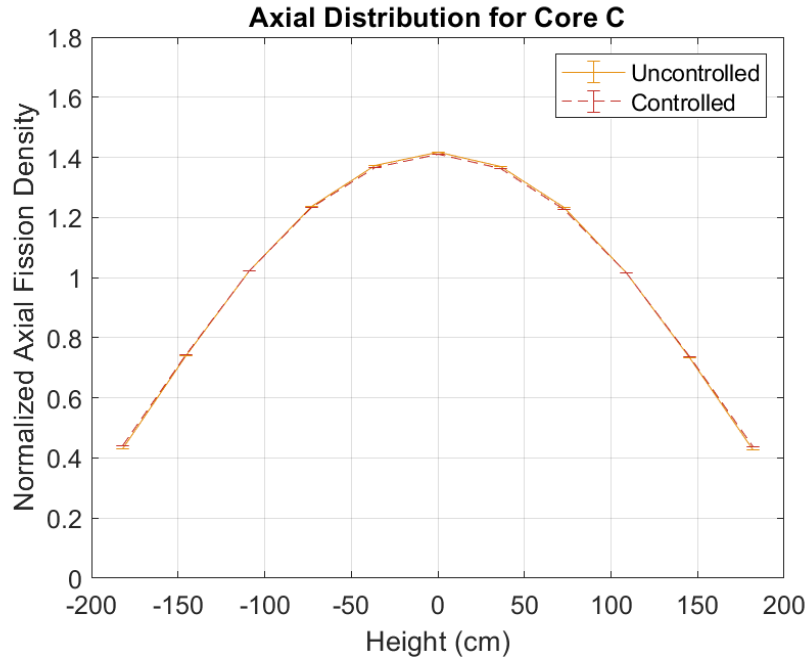


**Figure 23. Axial Fission Density Distribution for Core C**

All configurations across all cores, except the near-critical configuration of core B, have nearly-identical axial distributions. This result is expected as the core is axially uniform in all cases except the near-critical core B, where several assemblies have partially inserted control rods. The impact of this is shown in Figure 22, where significant bottom peaking can be observed in the core.

#### 4.4 Assembly-Averaged 11-Division Relative Fission Density Results

The assembly-averaged relative fission density values for each 1/11<sup>th</sup> axial division in the full core for uncontrolled, controlled, and near-critical cases are provided for control rod option A and B below in Table IV - Table IX. Additionally, the assembly-averaged relative fission densities for each 1/11<sup>th</sup> division in the core for uncontrolled and controlled cases are provided for control rod option C below in Table X and Table XI, respectively. In the tables below, division 1 below represents the lowest 1/11<sup>th</sup> division of the 4-meter

core, progressing up to division 11 which represents the axially highest 1/11<sup>th</sup> region of the core. A color scale is formatted on to each plot to identify the highest values in red and lowest values in blue. Figure 24 below provides the assembly indices for the core to reference in the tables below. For brevity, only the ranges of statistical uncertainties are provided underneath each table instead of individual uncertainties for each value. The uncertainty for each individual 1/11<sup>th</sup> assembly-averaged relative fission density is presented alongside its respective value in the detailed electronic file attachments provided with the thesis online in addition to the 1/11<sup>th</sup> pin relative fission densities for all single assembly and full core configurations.

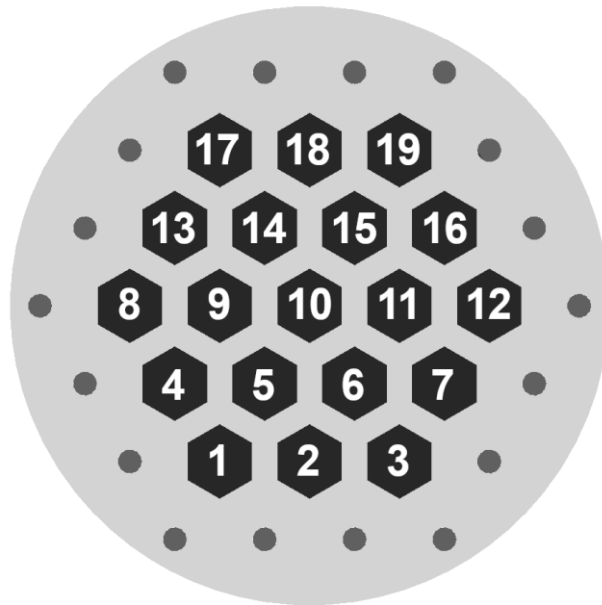


**Figure 24. Stylized Core Cross Section with Assembly Indices**

**Table IV. 1/11<sup>th</sup> Assembly-Avg. Relative Fission Densities - Uncontrolled Core A**

		Axial Division Number										
		1	2	3	4	5	6	7	8	9	10	11
Assembly Number	1	0.335	0.576	0.798	0.966	1.074	1.109	1.073	0.966	0.795	0.575	0.336
	2	0.393	0.678	0.934	1.130	1.259	1.301	1.260	1.139	0.939	0.681	0.395
	3	0.334	0.576	0.797	0.966	1.072	1.109	1.074	0.968	0.800	0.578	0.334
	4	0.397	0.681	0.940	1.139	1.265	1.302	1.262	1.141	0.942	0.680	0.395
	5	0.529	0.903	1.246	1.507	1.672	1.732	1.673	1.513	1.248	0.906	0.531
	6	0.530	0.901	1.247	1.507	1.675	1.734	1.678	1.512	1.249	0.906	0.528
	7	0.395	0.679	0.939	1.136	1.259	1.304	1.260	1.139	0.938	0.682	0.395
	8	0.337	0.580	0.801	0.966	1.070	1.108	1.075	0.970	0.801	0.581	0.336
	9	0.531	0.906	1.247	1.510	1.678	1.737	1.679	1.516	1.253	0.911	0.533
	10	0.611	1.043	1.435	1.738	1.930	2.001	1.936	1.745	1.444	1.051	0.615
	11	0.529	0.905	1.248	1.513	1.675	1.732	1.676	1.512	1.251	0.907	0.532
	12	0.336	0.578	0.801	0.970	1.073	1.107	1.074	0.969	0.798	0.578	0.336
	13	0.397	0.682	0.939	1.137	1.261	1.307	1.267	1.140	0.942	0.684	0.397
	14	0.530	0.906	1.249	1.514	1.676	1.733	1.681	1.514	1.254	0.910	0.533
	15	0.529	0.905	1.246	1.506	1.678	1.735	1.679	1.513	1.256	0.910	0.531
	16	0.396	0.682	0.944	1.140	1.261	1.304	1.264	1.140	0.944	0.684	0.397
	17	0.337	0.580	0.799	0.966	1.071	1.108	1.076	0.974	0.803	0.581	0.336
	18	0.396	0.681	0.940	1.138	1.263	1.305	1.262	1.141	0.946	0.686	0.397
	19	0.335	0.577	0.799	0.970	1.075	1.109	1.075	0.971	0.802	0.581	0.337

*1-Sigma Uncertainty Range: 0.0457% - 0.1141%*

**Table V. 1/11<sup>th</sup> Assembly-Avg. Relative Fission Densities - Controlled Core – A**

		Axial Division Number										
		1	2	3	4	5	6	7	8	9	10	11
<b>Assembly Number</b>	<b>1</b>	0.337	0.583	0.809	0.983	1.091	1.126	1.089	0.981	0.809	0.586	0.340
	<b>2</b>	0.396	0.681	0.946	1.147	1.270	1.314	1.270	1.146	0.946	0.684	0.400
	<b>3</b>	0.337	0.584	0.808	0.979	1.086	1.124	1.090	0.983	0.807	0.584	0.340
	<b>4</b>	0.398	0.682	0.945	1.145	1.270	1.314	1.271	1.146	0.947	0.685	0.398
	<b>5</b>	0.524	0.890	1.233	1.495	1.659	1.718	1.657	1.494	1.231	0.893	0.529
	<b>6</b>	0.522	0.891	1.234	1.497	1.661	1.718	1.660	1.498	1.233	0.894	0.527
	<b>7</b>	0.396	0.681	0.941	1.144	1.268	1.312	1.275	1.151	0.947	0.684	0.399
	<b>8</b>	0.338	0.585	0.810	0.982	1.093	1.130	1.089	0.982	0.809	0.586	0.340
	<b>9</b>	0.525	0.891	1.235	1.497	1.662	1.716	1.658	1.495	1.236	0.894	0.527
	<b>10</b>	0.601	1.023	1.414	1.719	1.906	1.971	1.903	1.715	1.412	1.028	0.605
	<b>11</b>	0.525	0.894	1.233	1.496	1.664	1.722	1.664	1.499	1.233	0.894	0.525
	<b>12</b>	0.339	0.586	0.811	0.983	1.094	1.131	1.097	0.984	0.811	0.584	0.339
	<b>13</b>	0.399	0.683	0.946	1.150	1.274	1.314	1.271	1.146	0.945	0.685	0.397
	<b>14</b>	0.525	0.893	1.233	1.495	1.662	1.716	1.657	1.494	1.234	0.894	0.526
	<b>15</b>	0.525	0.892	1.229	1.495	1.661	1.719	1.661	1.497	1.236	0.893	0.527
	<b>16</b>	0.399	0.684	0.947	1.146	1.277	1.320	1.276	1.148	0.943	0.684	0.399
	<b>17</b>	0.339	0.585	0.810	0.980	1.093	1.124	1.085	0.980	0.812	0.588	0.341
	<b>18</b>	0.398	0.684	0.942	1.147	1.272	1.312	1.274	1.150	0.949	0.687	0.401
	<b>19</b>	0.340	0.584	0.809	0.981	1.095	1.127	1.094	0.988	0.815	0.587	0.342

*1-Sigma Uncertainty Range: 0.0504% - 0.1239%*

**Table VI. 1/11<sup>th</sup> Assembly-Avg. Relative Fission Densities - Near-Critical Core – A**

		Axial Division Number										
		1	2	3	4	5	6	7	8	9	10	11
Assembly Number	1	0.339	0.589	0.816	0.988	1.093	1.126	1.088	0.982	0.806	0.581	0.336
	2	0.504	0.886	1.226	1.482	1.634	1.690	1.641	1.476	1.216	0.875	0.500
	3	0.337	0.589	0.814	0.988	1.089	1.127	1.091	0.982	0.807	0.580	0.334
	4	0.503	0.881	1.224	1.486	1.640	1.691	1.633	1.475	1.213	0.875	0.501
	5	0.441	0.750	1.039	1.262	1.396	1.434	1.390	1.254	1.031	0.744	0.440
	6	0.444	0.751	1.038	1.258	1.395	1.437	1.390	1.250	1.029	0.743	0.437
	7	0.505	0.880	1.221	1.482	1.642	1.694	1.636	1.471	1.213	0.870	0.498
	8	0.337	0.586	0.814	0.987	1.088	1.123	1.088	0.981	0.807	0.582	0.335
	9	0.442	0.748	1.038	1.260	1.395	1.435	1.387	1.251	1.030	0.743	0.439
	10	0.440	0.735	1.013	1.232	1.362	1.403	1.357	1.219	1.007	0.729	0.437
	11	0.443	0.747	1.036	1.256	1.389	1.434	1.388	1.248	1.031	0.743	0.439
	12	0.336	0.584	0.812	0.980	1.089	1.128	1.088	0.978	0.809	0.582	0.336
	13	0.504	0.879	1.222	1.481	1.640	1.691	1.630	1.471	1.213	0.873	0.499
	14	0.443	0.749	1.036	1.258	1.394	1.438	1.389	1.247	1.030	0.745	0.439
	15	0.441	0.748	1.035	1.253	1.393	1.435	1.387	1.250	1.031	0.747	0.440
	16	0.504	0.876	1.214	1.472	1.637	1.689	1.637	1.475	1.219	0.879	0.503
	17	0.339	0.584	0.812	0.987	1.093	1.125	1.088	0.980	0.808	0.582	0.334
	18	0.505	0.878	1.220	1.478	1.643	1.691	1.634	1.472	1.215	0.874	0.499
	19	0.338	0.585	0.810	0.982	1.092	1.124	1.089	0.979	0.810	0.583	0.337

*1-Sigma Uncertainty Range: 0.0538% - 0.1209%*

**Table VII. 1/11<sup>th</sup> Assembly-Avg. Relative Fission Densities - Uncontrolled Core – B**

		Axial Division Number										
		1	2	3	4	5	6	7	8	9	10	11
Assembly Number	1	0.337	0.579	0.799	0.971	1.075	1.113	1.077	0.970	0.802	0.580	0.335
	2	0.396	0.680	0.943	1.141	1.262	1.304	1.263	1.142	0.939	0.680	0.393
	3	0.335	0.578	0.798	0.968	1.071	1.109	1.073	0.967	0.795	0.576	0.334
	4	0.397	0.681	0.940	1.140	1.263	1.307	1.264	1.140	0.942	0.680	0.395
	5	0.531	0.905	1.250	1.516	1.682	1.737	1.677	1.508	1.246	0.904	0.528
	6	0.529	0.906	1.250	1.512	1.676	1.732	1.674	1.511	1.249	0.903	0.529
	7	0.397	0.683	0.940	1.140	1.261	1.302	1.260	1.136	0.937	0.677	0.394
	8	0.336	0.578	0.799	0.969	1.072	1.113	1.077	0.968	0.802	0.579	0.335
	9	0.532	0.908	1.253	1.516	1.679	1.735	1.677	1.510	1.248	0.903	0.527
	10	0.614	1.045	1.445	1.747	1.935	1.995	1.931	1.738	1.438	1.042	0.610
	11	0.531	0.907	1.252	1.515	1.678	1.735	1.676	1.509	1.249	0.903	0.526
	12	0.336	0.581	0.803	0.973	1.073	1.107	1.071	0.968	0.800	0.577	0.334
	13	0.396	0.682	0.941	1.141	1.266	1.302	1.262	1.137	0.936	0.679	0.395
	14	0.532	0.908	1.254	1.517	1.681	1.731	1.679	1.507	1.248	0.904	0.529
	15	0.531	0.910	1.256	1.518	1.679	1.732	1.677	1.511	1.245	0.899	0.528
	16	0.398	0.688	0.944	1.139	1.265	1.307	1.257	1.136	0.938	0.676	0.394
	17	0.335	0.579	0.799	0.973	1.078	1.110	1.075	0.968	0.798	0.576	0.334
	18	0.395	0.681	0.942	1.144	1.268	1.307	1.262	1.133	0.934	0.678	0.394
	19	0.335	0.583	0.804	0.971	1.073	1.112	1.070	0.963	0.797	0.576	0.334

*1-Sigma Uncertainty Range: 0.0459% - 0.1140%*

**Table VIII. 1/11<sup>th</sup> Assembly-Avg. Relative Fission Densities - Controlled Core – B**

		Axial Division Number										
		1	2	3	4	5	6	7	8	9	10	11
Assembly Number	1	0.348	0.576	0.789	0.951	1.051	1.085	1.052	0.949	0.785	0.572	0.344
	2	0.416	0.684	0.939	1.127	1.243	1.284	1.242	1.118	0.925	0.679	0.411
	3	0.351	0.580	0.793	0.955	1.055	1.084	1.050	0.944	0.784	0.578	0.347
	4	0.411	0.682	0.934	1.124	1.245	1.289	1.242	1.120	0.926	0.681	0.414
	5	0.564	0.926	1.265	1.522	1.686	1.739	1.681	1.513	1.253	0.921	0.560
	6	0.567	0.928	1.269	1.522	1.680	1.734	1.678	1.514	1.257	0.921	0.560
	7	0.417	0.686	0.939	1.126	1.241	1.282	1.240	1.118	0.930	0.684	0.412
	8	0.348	0.576	0.787	0.952	1.050	1.087	1.048	0.946	0.784	0.576	0.348
	9	0.562	0.922	1.261	1.526	1.691	1.739	1.683	1.514	1.259	0.921	0.561
	10	0.654	1.073	1.462	1.763	1.955	2.017	1.948	1.756	1.459	1.067	0.649
	11	0.564	0.926	1.266	1.522	1.679	1.735	1.678	1.514	1.259	0.924	0.559
	12	0.349	0.578	0.790	0.949	1.047	1.082	1.044	0.944	0.789	0.577	0.349
	13	0.410	0.683	0.935	1.125	1.250	1.283	1.240	1.122	0.929	0.680	0.411
	14	0.561	0.923	1.264	1.520	1.689	1.736	1.677	1.518	1.257	0.920	0.561
	15	0.563	0.924	1.262	1.521	1.678	1.734	1.679	1.513	1.259	0.920	0.559
	16	0.417	0.686	0.936	1.124	1.245	1.277	1.236	1.122	0.937	0.684	0.410
	17	0.345	0.573	0.789	0.951	1.052	1.086	1.048	0.950	0.788	0.579	0.347
	18	0.412	0.683	0.935	1.126	1.246	1.284	1.237	1.122	0.933	0.679	0.411
	19	0.348	0.577	0.788	0.953	1.049	1.080	1.050	0.947	0.785	0.572	0.345

*1-Sigma Uncertainty Range: 0.0503% - 0.1250%*

**Table IX. 1/11<sup>th</sup> Assembly-Avg. Relative Fission Densities - Near-Critical Core – B**

		Axial Division Number										
		1	2	3	4	5	6	7	8	9	10	11
Assembly Number	1	0.579	0.979	1.304	1.500	1.559	1.463	1.233	0.899	0.541	0.289	0.130
	2	0.482	0.784	1.043	1.200	1.247	1.170	0.986	0.712	0.430	0.226	0.104
	3	0.320	0.512	0.678	0.779	0.807	0.757	0.641	0.475	0.301	0.167	0.078
	4	0.481	0.781	1.044	1.204	1.244	1.170	0.982	0.711	0.424	0.224	0.104
	5	0.940	1.569	2.092	2.414	2.500	2.343	1.964	1.373	0.654	0.316	0.139
	6	0.879	1.462	1.947	2.241	2.318	2.174	1.823	1.299	0.739	0.376	0.166
	7	0.479	0.781	1.040	1.203	1.245	1.169	0.981	0.712	0.427	0.225	0.103
	8	0.317	0.509	0.678	0.780	0.806	0.757	0.639	0.471	0.298	0.164	0.079
	9	0.878	1.455	1.947	2.243	2.321	2.177	1.828	1.298	0.732	0.372	0.167
	10	0.913	1.499	1.994	2.299	2.379	2.233	1.867	1.321	0.727	0.359	0.160
	11	0.937	1.568	2.090	2.412	2.499	2.340	1.960	1.371	0.655	0.315	0.138
	12	0.576	0.971	1.302	1.499	1.552	1.458	1.232	0.898	0.539	0.287	0.129
	13	0.480	0.784	1.046	1.202	1.245	1.171	0.987	0.711	0.424	0.223	0.103
	14	0.937	1.569	2.092	2.417	2.494	2.346	1.963	1.370	0.651	0.314	0.139
	15	0.878	1.461	1.943	2.237	2.319	2.176	1.825	1.299	0.736	0.373	0.167
	16	0.480	0.784	1.039	1.201	1.244	1.168	0.983	0.712	0.426	0.223	0.103
	17	0.576	0.972	1.298	1.504	1.554	1.462	1.234	0.896	0.538	0.286	0.129
	18	0.480	0.784	1.044	1.203	1.245	1.172	0.985	0.714	0.425	0.224	0.103
	19	0.320	0.510	0.675	0.781	0.808	0.759	0.640	0.474	0.300	0.164	0.078

*1-Sigma Uncertainty Range: 0.0435% - 0.2460%*

**Table X. 1/11<sup>th</sup> Assembly-Avg. Relative Fission Densities - Uncontrolled Core – C**

		Axial Division Number										
		1	2	3	4	5	6	7	8	9	10	11
Assembly Number	1	0.336	0.579	0.800	0.971	1.076	1.112	1.075	0.967	0.796	0.574	0.331
	2	0.394	0.682	0.943	1.143	1.268	1.310	1.265	1.134	0.937	0.675	0.392
	3	0.332	0.576	0.799	0.968	1.076	1.109	1.075	0.966	0.798	0.575	0.333
	4	0.395	0.683	0.941	1.141	1.269	1.308	1.267	1.137	0.936	0.676	0.392
	5	0.531	0.909	1.252	1.519	1.687	1.743	1.681	1.511	1.249	0.902	0.527
	6	0.531	0.907	1.252	1.514	1.684	1.738	1.680	1.513	1.247	0.901	0.528
	7	0.394	0.680	0.939	1.140	1.266	1.305	1.261	1.137	0.935	0.676	0.393
	8	0.334	0.578	0.798	0.968	1.071	1.109	1.071	0.964	0.795	0.576	0.332
	9	0.530	0.910	1.253	1.518	1.685	1.738	1.680	1.513	1.245	0.900	0.526
	10	0.612	1.044	1.443	1.747	1.935	2.007	1.936	1.744	1.440	1.042	0.610
	11	0.531	0.907	1.253	1.518	1.685	1.738	1.677	1.512	1.250	0.903	0.528
	12	0.334	0.578	0.800	0.970	1.074	1.110	1.069	0.967	0.798	0.576	0.333
	13	0.397	0.681	0.941	1.145	1.268	1.307	1.262	1.134	0.934	0.675	0.394
	14	0.530	0.907	1.251	1.516	1.682	1.738	1.679	1.513	1.248	0.903	0.529
	15	0.529	0.906	1.253	1.516	1.684	1.741	1.679	1.511	1.250	0.904	0.528
	16	0.394	0.680	0.940	1.143	1.266	1.305	1.259	1.138	0.939	0.678	0.394
	17	0.335	0.579	0.800	0.968	1.073	1.110	1.073	0.966	0.794	0.572	0.333
	18	0.397	0.683	0.942	1.141	1.262	1.303	1.264	1.136	0.938	0.675	0.392
	19	0.335	0.579	0.801	0.969	1.074	1.106	1.070	0.964	0.795	0.574	0.332

*1-Sigma Uncertainty Range: 0.0458% - 0.1144%*

**Table XI. 1/11<sup>th</sup> Assembly-Avg. Relative Fission Densities - Controlled Core – C**

		Axial Division Number										
		1	2	3	4	5	6	7	8	9	10	11
Assembly Number	1	0.338	0.569	0.785	0.947	1.053	1.089	1.055	0.944	0.780	0.570	0.338
	2	0.406	0.684	0.941	1.140	1.265	1.301	1.259	1.136	0.939	0.683	0.406
	3	0.353	0.601	0.828	0.995	1.101	1.139	1.102	0.995	0.821	0.599	0.352
	4	0.408	0.688	0.944	1.140	1.266	1.309	1.264	1.138	0.938	0.680	0.404
	5	0.541	0.904	1.240	1.496	1.658	1.712	1.655	1.491	1.231	0.896	0.535
	6	0.540	0.907	1.247	1.505	1.666	1.715	1.661	1.496	1.235	0.899	0.538
	7	0.407	0.689	0.947	1.142	1.266	1.305	1.262	1.135	0.941	0.681	0.404
	8	0.355	0.601	0.825	0.997	1.106	1.144	1.109	0.998	0.824	0.597	0.352
	9	0.544	0.908	1.243	1.504	1.666	1.723	1.665	1.497	1.240	0.902	0.534
	10	0.623	1.044	1.429	1.722	1.912	1.972	1.903	1.713	1.417	1.031	0.618
	11	0.542	0.905	1.244	1.501	1.660	1.715	1.660	1.495	1.236	0.900	0.537
	12	0.340	0.575	0.789	0.956	1.056	1.088	1.051	0.947	0.785	0.571	0.336
	13	0.409	0.689	0.943	1.140	1.266	1.309	1.267	1.140	0.942	0.684	0.405
	14	0.539	0.907	1.243	1.497	1.662	1.713	1.655	1.494	1.234	0.898	0.535
	15	0.542	0.907	1.249	1.502	1.671	1.721	1.660	1.493	1.236	0.897	0.536
	16	0.409	0.688	0.947	1.145	1.263	1.306	1.263	1.138	0.939	0.681	0.403
	17	0.340	0.574	0.789	0.955	1.056	1.089	1.051	0.948	0.784	0.571	0.338
	18	0.407	0.688	0.948	1.143	1.267	1.307	1.261	1.133	0.938	0.682	0.406
	19	0.354	0.603	0.830	1.002	1.110	1.146	1.106	0.995	0.822	0.596	0.352

*1-Sigma Uncertainty Range: 0.0488% - 0.1208%*

## **CHAPTER 5. FUTURE WORK**

The next step beyond the work presented in this thesis for steady-state neutronic benchmarking is to develop the stylized design further into a time-dependent thermal-fluid coupled fresh core benchmark. This coupled benchmark will likely feature a smaller-scale problem only (e.g., single-assembly scale) due to the complexity of the problem and the fact the computational burden will be prohibitive for a full-core model. Development of single physics time dependent benchmark problems and their corresponding solutions for neutronics and thermal fluids separately must be the next immediate step.

## APPENDIX A. SUMMARY OF ATTACHED FILES

The results for each case presented are attached in a variety of forms to maximize the utility and ease of access for the data. Additionally, every continuous energy MCNP5<sup>2</sup> input is attached to run directly or to be used as a reference when building an input for a different program. Below, a summary of each attached file is provided and how to best utilize them.

### A.1 Input Files

The input files created for the stylized SmaHTR benchmark set are compressed into a .zip file titled [SmaHTR\\_Reed\\_Inputs.zip](#). This .zip file contains the following inputs arranged in Table XII below. The abbreviations for file notation are noted below the table.

**Table XII. Input File Summary**

	3-D Inputs		
	Case A	Case B	Case C
Single Assembly	SA_A_UC.i SA_A_CT.i	SA_B_UC.i SA_B_CT.i	SA_C_UC.i SA_C_CT.i
Full Core	FC_A_UC.i FC_A_CT.i FC_A_Crt.i	FC_B_UC.i FC_B_CT.i FC_B_Crt.i	FC_C_UC.i FC_C_CT.i

**SA** = Single Assembly

**FC** = Full Core

**\_A** = Control Option A

**\_B** = Control Option B

**\_C** = Control Option C

**\_UC** = Uncontrolled Case

**\_CT** = Controlled Case

**\_Crt** = Near-Critical Case

## A.2 Data Files

The data files available for download with this thesis are summarized in below with their titles and content summary. The data is organized into several different Excel files within [SmAHTR\\_Reed\\_Data.zip](#) by the notation in Table XIII below.

**Table XIII. Data File Summary**

	3-D Inputs		
	Case A	Case B	Case C
Single Assembly	SA_A.xlsx	SA_B.xlsx	SA_C.xlsx
Full Core	FC_A_UC.xlsx FC_A_CT.xlsx FC_A_Crt.xlsx	FC_B_UC.xlsx FC_B_CT.xlsx FC_B_Crt.xlsx	FC_C_UC.xlsx FC_C_CT.xlsx

**SA** = Single Assembly      **FC** = Full Core

**\_A** = Control Option A      **\_B** = Control Option B      **\_C** = Control Option C

**\_UC** = Uncontrolled Case      **\_CT** = Controlled Case      **\_Crt** = Near-Critical Case

For 3-D Single Assembly options A, B, and C, the following are provided for both uncontrolled and controlled cases within each file:

- 1/11<sup>th</sup> Pin Relative Fission Density Values and Uncertainties
- Assembly Radial Relative Fission Density Values and Uncertainties
- Assembly Axial Relative Fission Density Values and Uncertainties

For 3-D Full Core options A, B, and C for each configuration, the following data are provided within each file:

- 1/11<sup>th</sup> Pin Relative Fission Density Values and Uncertainties
- 1/11<sup>th</sup> Assembly-Averaged Relative Fission Density Values and Uncertainties
- Full Core Radial Relative Fission Density Values and Uncertainties
- Full Core Axial Relative Fission Density Values and Uncertainties

## REFERENCES

- [1] Greene et al. (2011). *Pre-Conceptual Design of a Fluoride-Salt-Cooled Small Modular Advanced High Temperature Reactor (SMAHTR)*. Oak Ridge, TN: Oak Ridge National Laboratory. doi:10.2172/1008830
- [2] X-5 Monte Carlo Team. (2003). *MCNP—Version 5, Vol. I: Overview and Theory*. LA-UR-03-1987, Los Alamos National Laboratory.
- [3] K. Reed, F. Rahnema. (2020). A Simplified SMAHTR Benchmark Problem Set. *Proceedings of PHYSOR 2020 - Transition to a Scalable Nuclear Future*. Cambridge, United Kingdom.
- [4] D. Zhang, F. Rahnema. (2018). A Stylized 3D Advanced High Temperature Reactor (AHTR) Benchmark Problem. *Annals of Nuclear Energy*, 120, 178-185. Retrieved from <https://doi.org/10.1016/j.anucene.2018.05.019>
- [5] S. Chandrasekaran, S. Garimella. (2020). Steady-State Thermal-Hydraulic Model for Fluoride-Salt-Cooled Small Modular High-Temperature Reactors. *Nuclear Technology*. doi:10.1080/00295450.2020.1750274
- [6] K. Connolly, F. Rahnema, P. Tsvetkov. (2015). Prismatic VHTR Neutronic Benchmark Problems. *Nuclear Engineering and Design*, 285, 207-240. doi:10.1016/j.nucengdes.2014.11.044
- [7] B. Collin. (2014). *AGR-2 Irradiation Test Final As-Run Report, Rev 2*. Idaho National Laboratory. doi:10.2172/1167549

- [8] D. Ilas, J. C. Gehin. (2010). HTTR Fuel Block Simulations with SCALE. *Proceedings of PHYSOR 2010 – Advances in Reactor Physics to Power the Nuclear Renaissance*. Pittsburgh, PA.